SKBF
KBS
TEKNISK
RAPPORT
82-07

Copper/bentonite interaction

Roland Pusch

Division Soil Mechanics, University, University of Luleå
Luleå, Sweden, 1982-06-30

SVENSK KÄRNBRÄNSLEFÖRSÖRJNING AB / AVDELNING KBS

POSTADRESS: Box 5864, 102 48 Stockholm, Telefon 08-67 95 40

COPPER/BENTONITE INTERACTION

Roland Pusch
Division Soil Mechanics
University of Luleå
Luleå, Sweden, 1982-06-30

A list of other reports published in this series during 1982, is attached at the end of this report. Information on KBS technical reports from 1977-1978 (TR 121), 1979 (TR 79-28), 1980 (TR 80-26) and 1981 (TR 81-17) is available through SKBF/KBS.

COPPER/BENTONITE INTERACTION

ROLAND PUSCH
DIV SOIL MECHANICS
UNIV OF LULEÅ

LULEÅ 820630

CONTENTS PAGE

Summary

The prediction of the processes and rate of corrosion of the KBS 2 copper canisters must be based on a proper scenario, which involves the physical state of the bentonite surrounding the canisters, and the chemical interaction between copper and bentonite. Literature data suggest slow Cu migration and Cu exchanging originally adsorbed cations. Two tests involving copper/bentonite contacts for 3 - 6 months in boreholes have yielded certain valuable information. Thus, Cu ion migration is indeed very slow and where it yields a sufficiently high concentration, it is associated with replacement of originally adsorbed Na ions, which should result in an increased permeability.

In one of the tests the copper was separated from the bentonite by a partly air-filled slot. These conditions caused the formation of copper oxides and hydroxides which intermingled with the bentonite that expanded to fill the slot. Due to the low solubility of these copper compounds, the Cu ion concentration was too low to produce ion exchange during the time of observation.

Scope of study

Not until the copper canisters of the KBS 2 concept have corroded to form paths for the confined radionuclides to leave the canisters, radioactivity will spread. The rate of corrosion is therefore of utmost importance, but in order to derive a model for its determination it is necessary firstly to define the "micro-environment" at the surface of the copper canisters. Since the copper will be in contact with clay (Na bentonite), the physical state of this substance and its interaction with copper will be of primary interest. This is the scope of the present study, which should be considered as a first phase of a more comprehensive investigation.

Main outlines of the KBS 2 concept

Arrangement and geometry of canister and clay buffer

Fig. 1 illustrates the general arrangement of a ϕ 0.78 m copper canister in its deposition hole, the diameter of which is 1.5 m. Closely fitting, precompacted Na bentonite blocks are applied to fill the space between the rock and the canister but for practical reasons an outer slot (a) and an inner slot (b) have to be left open. According to our present belief there are considerable advantages in filling the outer slot with water at the end of the application phase and it is assumed here that this procedure will be chosen in practice. "a" will be about 20-30 mm wide, while "b" will vary in the interval 0-5 mm.

The physico/chemical environment

The general scenario (cf. PUSCH, 1982) leading to corrosion of the copper canisters is assumed to be:

1. Air with a high relative humidity is initially present in the slot between the stack of highly compacted MX-80 bentonite blocks and the canister, as well as in the pores of the bentonite which has a degree of water saturation of about 60% at the deposition. Under these environmental conditions copper oxide and hydroxide compounds will be formed over the entire periphery of the canister. The heat production will yield a maximum surface temperature of the canister of about 90 ^{o}C, the gradient in the bentonite being about 1 ^{o}C per centimeter.

---

[1] Possibly the b-slot is going to be filled with fine-grained copper powder but this operation is not included in our scenario.

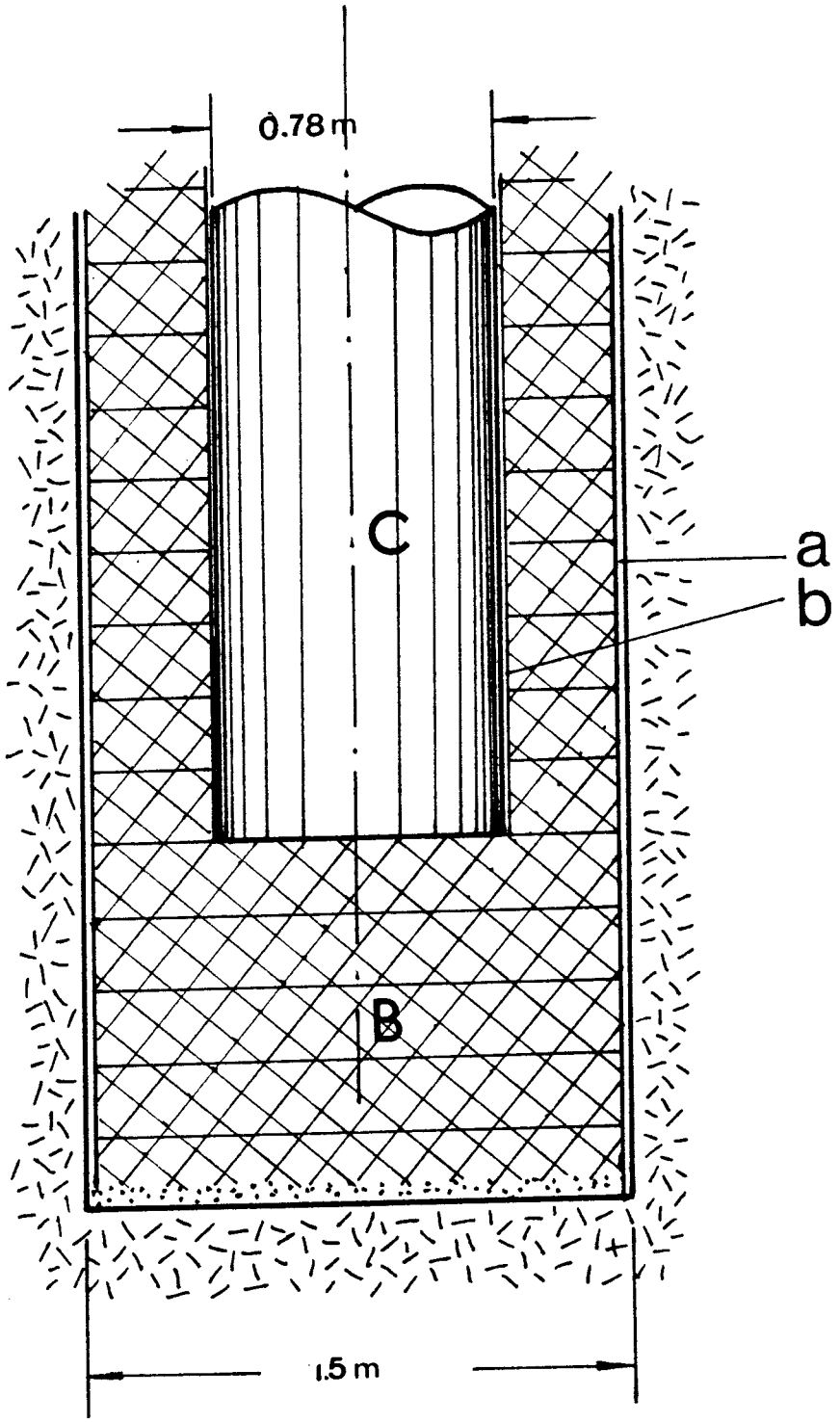

Fig. 1. The cylindrical copper canister in its clay envelope surrounded by rock. a is the outer slot, b the inner. B is the system of highly compacted bentonite blocks, while C is the copper canister.

2. In the normal case water will enter the bentonite blocks from the surrounding rock, which will make them swell and become saturated and thereby to expand to create a close contact and a swelling pressure of about 10 MPa. The bulk density at complete water saturation will be about 2.1 t/m^3, and the water content will be about 25%; the average pH ranging between 8 and 10. In rock with very few joints several hundred years may in fact be required to reach this state. Water saturation of the bentonite will cause the temperature to drop due to the increased heat conductivity.

3. The water uptake is due to the high affinity of montmorillonite to water. Montmorillonite is the active clay mineral in the bentonite, the crystal lattice being illustrated by Fig. 2 Parallel to and after the water saturation, the minerals and water molecules spontaneously redistribute themselves to yield a successively improved state of homogeneity (Fig. 3). The rather extreme specific surface area (700-800 m^2/g dry clay) means that the larger part of the pore water will be adsorbed and strongly held in interlamellar positions, i.e. in the 10-15 Å space between the 10Å thick crystal flake units. A certain small fraction of the pore water will, however, be located in more or less continuous passages ("voids") between clay particle aggregates. It will behave as free, bulk water and its pressure will be equal to the piezometric

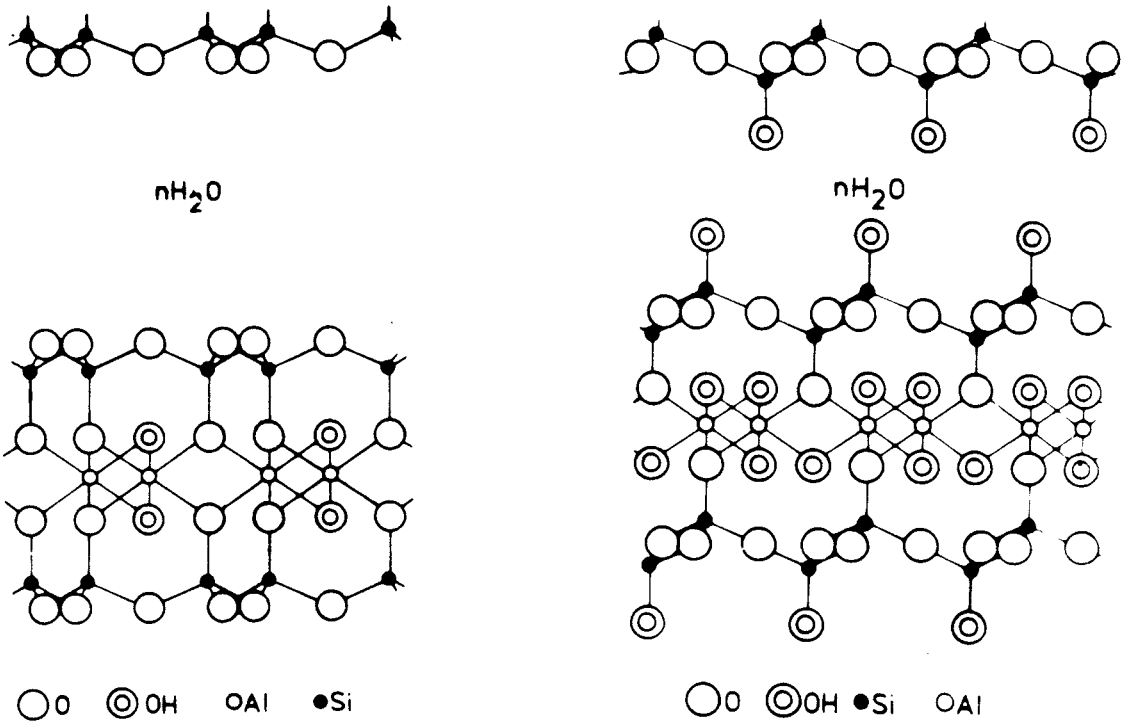

Fig. 2. Montmorillonite crystal structure models. Left: Hofmann, Endell & Wilm; Right: Edelman & Favajee. The latter seems to be valid, although with a reduced number of structural hydroxyls at the intra-aggregate basal planes, in the temperature range of the KBS 2 concept.

head in the repository; i.e. the pressure will depend on the groundwater level. The fact that water migrates towards the canister and that this process is associated with an expansion of the clay, means that water will in principle not be present in free form at the copper/clay interface; the canister will be contacted by a clay mass which strongly retains its pore water. One additional consequence of this is that the contact between the copper metal surface or, rather the previously formed coating of copper

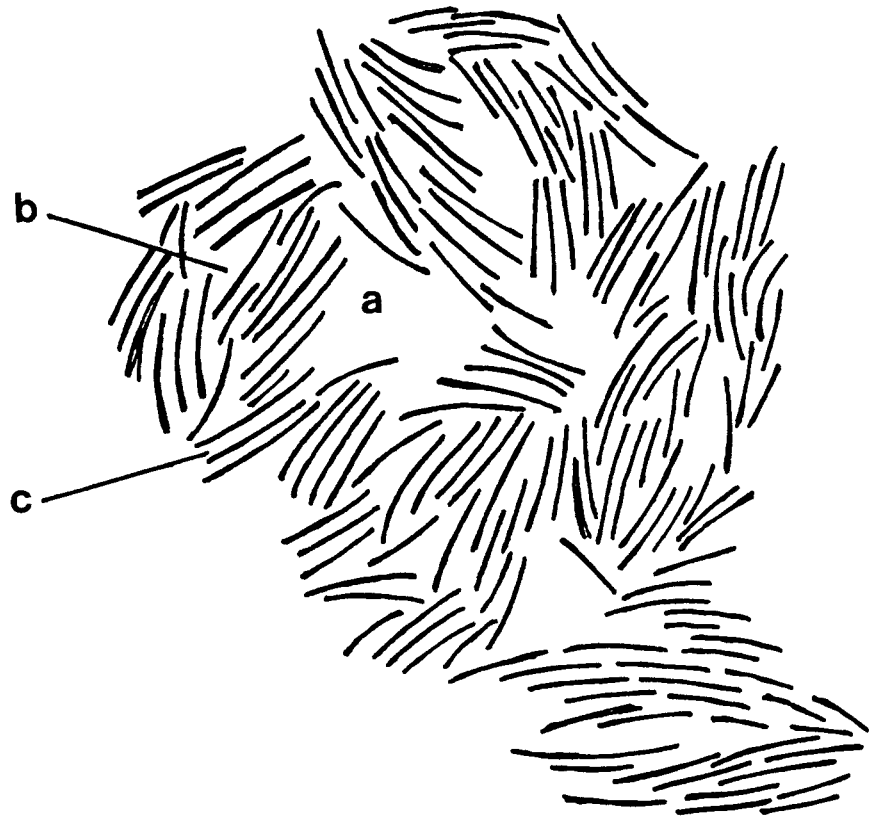

Fig. 3. Microstructural arrangement of 10Å montmorillonite flakes in "matured" water saturated Na bentonite. a) Large void (≥ 2 µm), b) Small void (≤ 0.2 µm), c) Intra-aggregate = interlamellar space (10-15 Å).

. oxide or hydroxide, and adjacent montmorillonite crystallites will be established through thin films of adsorbed water.

Cu-uptake in montmorillonite

Ion adsorption

The literature provides some information of how copper ions are adsorbed in montmorillonites. Thus, CLEMENTZ et al. (1974) concluded from comprehensive laboratory investigations

that copper (Cu^{2+}) can operate as an exchangeable ion, the predominant sites being external basal planes as well as interlamellar space, while edge sites are negligible. Their study involved ion exchange processes with dilute clay suspensions, which raises the question whether copper ions can migrate -through diffusion-into highly compacted bentonite as well. This will be discussed in a subsequent chapter.

CLEMENTS et al. showed that high surface charge montmorillonite corresponding to the KBS 2 concept with a low pore water salinity, takes up hydrated copper ions in interlamellar space which can expand further upon hydration. In low charge montmorillonite, i.e. the case of a pore water with high ionic strength, hydrated copper ions of the form $Cu(H_2O)^{2+}$ are probably present mainly on external basal planes. Since such exchange sites only form a small fraction of the total number of exchange positions, the uptake of copper in saline montmorillonite is probably negligible.

The copper ions in this study originated from $CuCl_2$ in 95% ethanol solution[1], which is known as an effective dispersing agent. It must be recalled that at pH higher than about 8 oxides, hydroxides, and carbonates of copper, being possible primary corrosion products of the waste canisters, are highly stable (KRAUSKOPF, 1956). This means that only a small fraction of the copper will be in ionic form at the canister/bentonite interface.

Effect of Cu-uptake on the physical properties of Na bentonite

The expected influence of Cu-uptake in highly compacted Na bentonite is a certain increase of the permeability, since a partial collapse of certain expanded aggregates in larger pores will probably take place upon the exchange of Na by Cu.

---

[1] It is not clear what effect different water/ethanol ratios would have, however.

The reduction can be assumed to be similar to that caused by exchange by Ca, which means that the permeability will be 2-5 times higher than in the Na state.[1)] The swelling pressure is not likely to be affected since it is found to be insensitive to pore water chemistry changes as long as the bulk density is higher than about 2 t/m^3. This is explained by the fact that electrical double-layers are not, or only partly developed in intra-aggregate space at these densities, and that the swelling pressure results from the integrated expansive forces exerted by the continuous network of particle aggregates and not from the clay gels in larger voids.

Experimental

General

No systematic study of the physical or chemical interaction of copper and bentonite has been conducted so far. The current KBS-directed research on the use of highly compacted bentonite for sealing purposes has offered a few opportunities, however, to observe how Cu is taken up in such clay under certain well defined experimental conditions. Two such cases will be referred to here; one being part of a test series conducted by Lars Werme, KBS, the other being related to a borehole sealing test under the guidance of the author.

Case I

This test was conducted in a tunnel in the Swedish Stripa mine at 350 m depth. A ø 56 mm borehole was equipped with a central stainless-steel pipe (outer diameter 20 mm) in which an electrical heater was inserted, and around which a sandwich column of a few millimeter thick alternating glass/ /metal discs separated by discs of highly compacted bentonite, was applied (Fig. 4). The copper (CuOFHC, Outukumpu) was of high purity; 99.99% Cu.

[1)] Cf. Pusch, 1982.

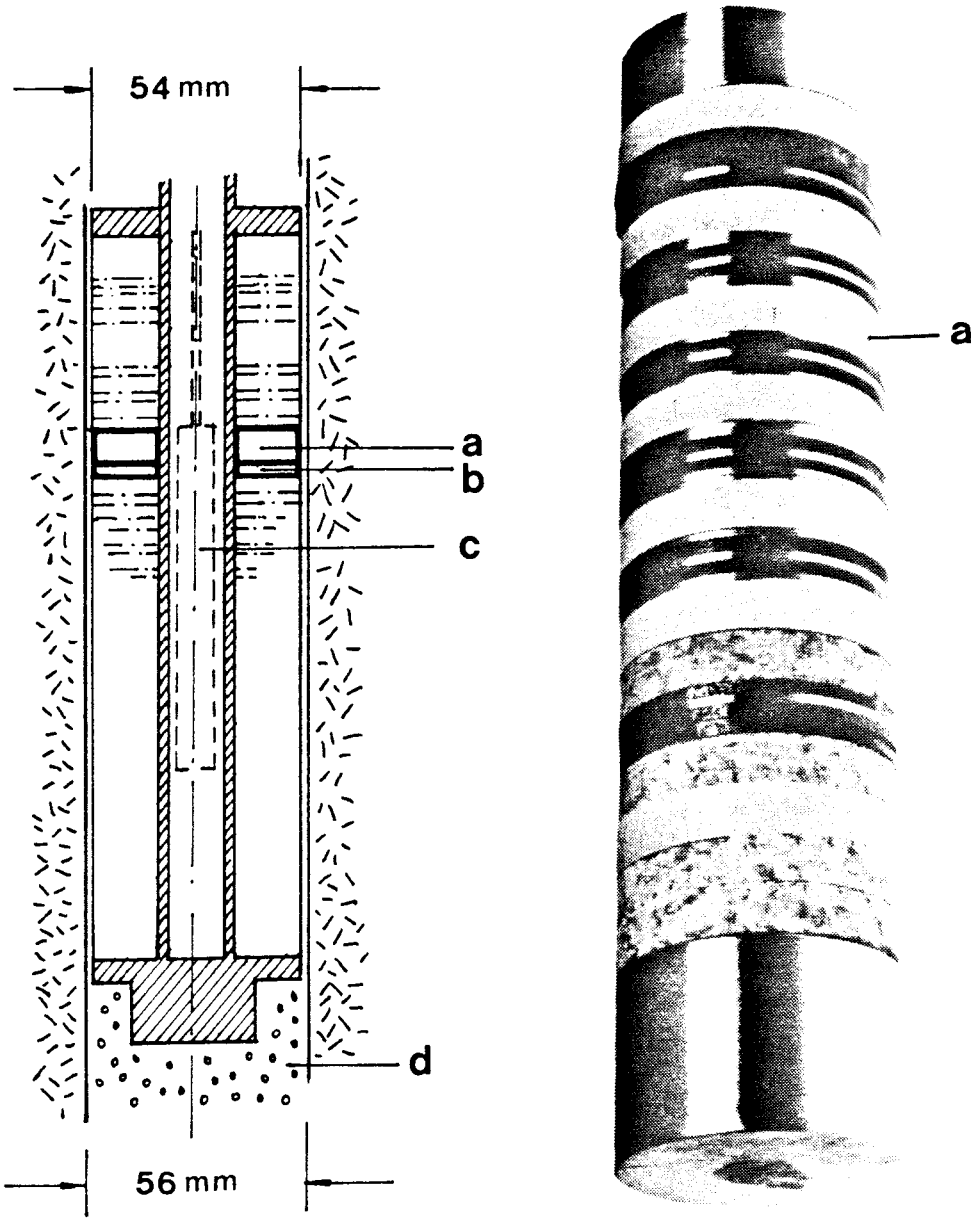

Fig. 4. Sandwich column consisting of a large number of metal and glass species and bentonite discs in the Stripa test. a) bentonite disc, b) copper disc, c) heater, d) sandfill in the lower part of the borehole. Only a limited number of sandwich constituents are shown. The photograph shows a sandwich with a slightly different base plate.

The hole was water-filled throughout the test, which lasted three months. It was filled, prior to the insertion of the sandwich structure, with groundwater from the close vicinity which had the following composition: pH=8.0, Ca=37 ppm, Mg=11 ppm, Na=8 ppm, K=2 ppm, Fe=0.3 ppm, Cl= 18 ppm, SO_4=32 ppm, and SiO_2= 9 ppm. The heater produced a constant temperature of 85 ^{o}C.

The sandwich was extracted from the hole with some difficulty because of the swelling of the bentonite. All voids and slots had been filled by the clay, the water content of the bentonite discs ranging between 28 and 33%[1]. The theoretical ultimate water content after complete water saturation and redistribution is about 35% corresponding to a bulk density of 1.9 t/m^3. This means that the clay had reached a high degree of water saturation in the course of the test.

One copper/bentonite unit was used for analys of the bentonite with respect to:

1. The X-ray diffraction characteristics[2]

   The equipment used was a Philips Automated Powder Diffractometer with a Cu long fine focus tube with maximum loading of 1.8 kW; normal run conditions were 40 kV, 30 mA. A theta-compensating slit permitted good resolution to 4$^{0}2\theta$. The computer was a NOVA 4/s; Philips software being used for the interpretation.

---

[1] The samples were stored too long after the extraction to make it possible to make reliable water content determinations. The values refer to parallel sandwich tests with the same geometry.

[2] All X-ray and element analyses were made by or through EMV Associates Inc. Microanalysis Laboratory, Rockville, Maryland USA.

Each sample was examined at the original interface and faces exposed at depths of 0, 0.05 mm, 1.0 mm, and 1.5 mm. These faces were exposed by cutting/ /scraping with a fine blade and then smoothing the resultant surface with a 220-grit silicon carbide abrasive. Remaining rough areas were masked to present even surfaces.

2. The element content by use of SEM/EDXA (Scanning electron microscopy and energy dispersive X-ray analysis);

   a) Use of single channel analyzer set for copper together with the SEM and EDXA to produce a graph of relative copper content as a function of distance from the interface along an analysis line.

   b) Use of SEM and EDXA to produce full area copper maps.

   c) Use of SEM and EDXA to produce micrographs and EDXA spectra at the following distances from the interface: 0, 0.1 mm, 0.2 mm, 0.3 mm, 0.4 mm, 1 mm, and 2 mm.

3. Results

   * The X-ray diffractograms (see Figs. 5-8) confirm that montmorillonite is the dominating mineral and that there are small amounts of quartz, feldspars and calcium carbonate, i.e. the expected composition of MX-80. The composition is unaltered by the nearness of the copper but there is a clear tendency for the (001) reflexion to be displaced close to the copper surface. Thus,

the characteristic strong peak of $2\theta \sim 6.9^{\circ}$ at 1.0 and 2 mm distance from this surface (D=12.8 to 12.9 Å) corresponds to $2\theta \sim 6.6^{\circ}$ (D~13.4 Å)and 6.5° at 0.5 and 0 mm distance from this interface, respectively. This expansion is probably due to a (partial) Cu occupation of interlamellar adsorption sites[1].

* The element analyses have been interpreted as follows (cf. Appendix 1).

a) The two copper line scans (Plate 1 and 2) show somewhat different patterns. Plate 1 indicates that the copper content varies irregularly all the way from the interface copper/bentonite (O-point), while the line scan of Plate 2 suggests a somewhat higher average Cu content within the first 1 mm interval than at larger distances from the interval. However, the peak height variation in the second scan does not indicate a definite Cu concentration gradient.

b) The full area copper maps show a fairly uniform distribution of a small number of very faint spots, indicating no Cu concentration gradient.

c) The examination of the micrographs showed the diagnostic feature of Na montmorillonite: the curly, flaky mass of interwoven laminae, and the same general microstructural pattern as water saturated virgin MX-80. Plates 3-9 show the presence of Si, Al, Fe, Ca, K, Ti, Cu, S, and Cl, the relative peak height [2] of copper being of primary interest. We see that

---

1) A verification of the Cu uptake could be achieved by performing chemical analyses by use of atomic adsorption technique as well.

2) Notice that the peak height refers to the peak extending above the background "horizon".

APD-3600 2ND DERIVATIVE PEAK ALGORITHM 1/20/82 13:44: 9

RAW DATA FILE : DPCA1.RD
SAMPLE ID : DPCA1
RAW DATA FILE DATE : 1/19/82
GENERATOR SETTINGS : 40 KV 30 MA
STEP SIZE, CNT TIME : 0.020 DEG 0.50 SEC
RANGE OF DATA : 2.000 - 70.000 DEG
RANGE IN D : 44.1372 - 1.3430 A
MAX PEAK CTS, CPS : 462. CTS 925. CPS
SECF APPLIED : NONE

2-THETA (DEG)	WIDTH (APPROX)	COUNTS PEAK	COUNTS BKGND	D (ANG)	I (NORM)	LINE TYPE a1	LINE TYPE a2	LINE TYPE BT	LINE TYPE AM	LINE TYPE OT
3.68	0.56	72.	142.	23.9905	15.63	X	X			
6.48	0.00	462.	25.	13.6397	100.00	U	U			
8.85	0.19	22.	52.	9.9783	4.78	X	X			
13.52	0.00	14.	48.	6.5416	3.12	U	U			
19.84	0.34	266.	81.	4.4714	57.48	X	X			
20.87	0.34	102.	92.	4.2530	22.07	X	X			
21.99	0.25	71.	106.	4.0397	15.26	X	X			
23.62	0.21	35.	114.	3.7637	7.53	X	X			
25.43	0.29	100.	110.	3.5004	21.63	X	X			
26.65	0.20	231.	110.	3.3416	49.98	X	X			
27.35	0.18	161.	110.	3.2583	34.89	X	X			
27.65	0.12	121.	110.	3.2230	26.18	X	X			
28.05	0.14	59.	110.	3.1780	12.83	X	X			
29.51	0.25	21.	98.	3.0240	4.58	X	X			
30.52	0.24	53.	96.	2.9267	11.53	X	X			
31.38	0.00	7.	98.	2.8480	1.46	U	U			
34.93	0.53	96.	88.	2.5663	20.78	X	X			
36.07	0.00	67.	90.	2.4877	14.55	U	U			
37.26	0.00	34.	94.	2.4116	7.28	U	U			
38.43	0.00	8.	92.	2.3408	1.82	U	U			

Fig. 5a. Recorded X-ray data for the copper/bentonite interface.

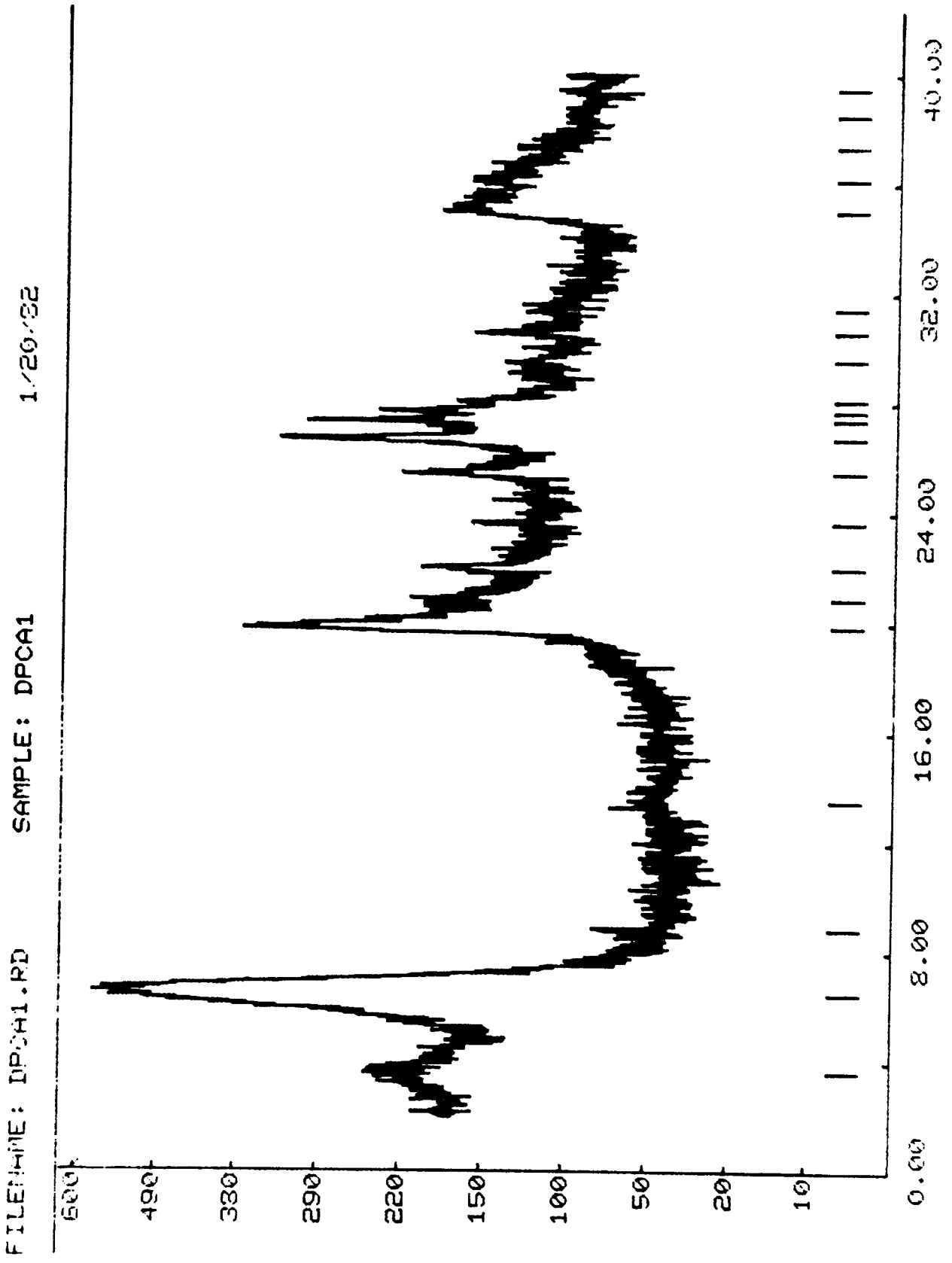

Fig. 5b. X-ray diffractogram for the copper/bentonite interface.

APD-3600 2ND DERIVATIVE PEAK ALGORITHM 1/20/82 13:44:56

RAW DATA FILE : DPCA2.RD
SAMPLE ID : DPCA2
RAW DATA FILE DATE : 1/19/82
GENERATOR SETTINGS : 40 KV 30 MA
STEP SIZE, CNT TIME : 0.020 DEG 0.50 SEC
RANGE OF DATA : 2.000 - 65.000 DEG
RANGE IN D : 44.1372 - 1.4337 A
MAX PEAK CTS, CPS : 177. CTS 354. CPS
SECF APPLIED : NONE

2-THETA (DEG)	WIDTH (APPROX)	COUNTS PEAK	COUNTS BKGND	D (ANG)	I (NORM)	LINE TYPE a1	LINE TYPE a2	LINE TYPE BT	LINE TYPE AM	LINE TYPE OT
6.59	0.00	156.	117.	13.4121	88.33	U	U			
8.78	0.00	19.	55.	10.0634	10.94	U	U			
13.66	0.00	18.	53.	6.4773	9.97	U	U			
19.77	0.27	177.	94.	4.4871	100.00	X	X			
21.94	0.31	49.	123.	4.0479	27.70	X	X			
25.46	0.27	28.	144.	3.4964	15.88	X	X			
26.60	0.25	121.	144.	3.3490	68.40	X	X			
27.71	0.25	108.	139.	3.2162	61.15	X	X			
28.04	0.16	90.	137.	3.1796	51.02	X	X			
29.49	0.31	12.	130.	3.0260	6.54	X	X			
30.36	0.36	28.	125.	2.9417	15.88	X	X			
35.10	0.30	72.	102.	2.5542	40.84	X	X			
42.21	0.25	14.	86.	2.1390	7.74	X	X			
50.08	0.39	18.	79.	1.8200	10.45	X	X			
50.90	0.34	7.	79.	1.7924	4.12	X	X			
54.13	0.00	28.	85.	1.6928	15.88	U	U			
57.44	0.19	11.	85.	1.6030	6.16	X	X			
61.93	0.52	32.	86.	1.4971	18.37	X	X			

18 PEAKS IDENTIFIED 18 CRYSTALLINE 0 AMORPHOUS
18 PEAKS LISTED

Fig. 6a. Recorded X-ray data for 0.5 mm distance from the copper/bentonite interface.

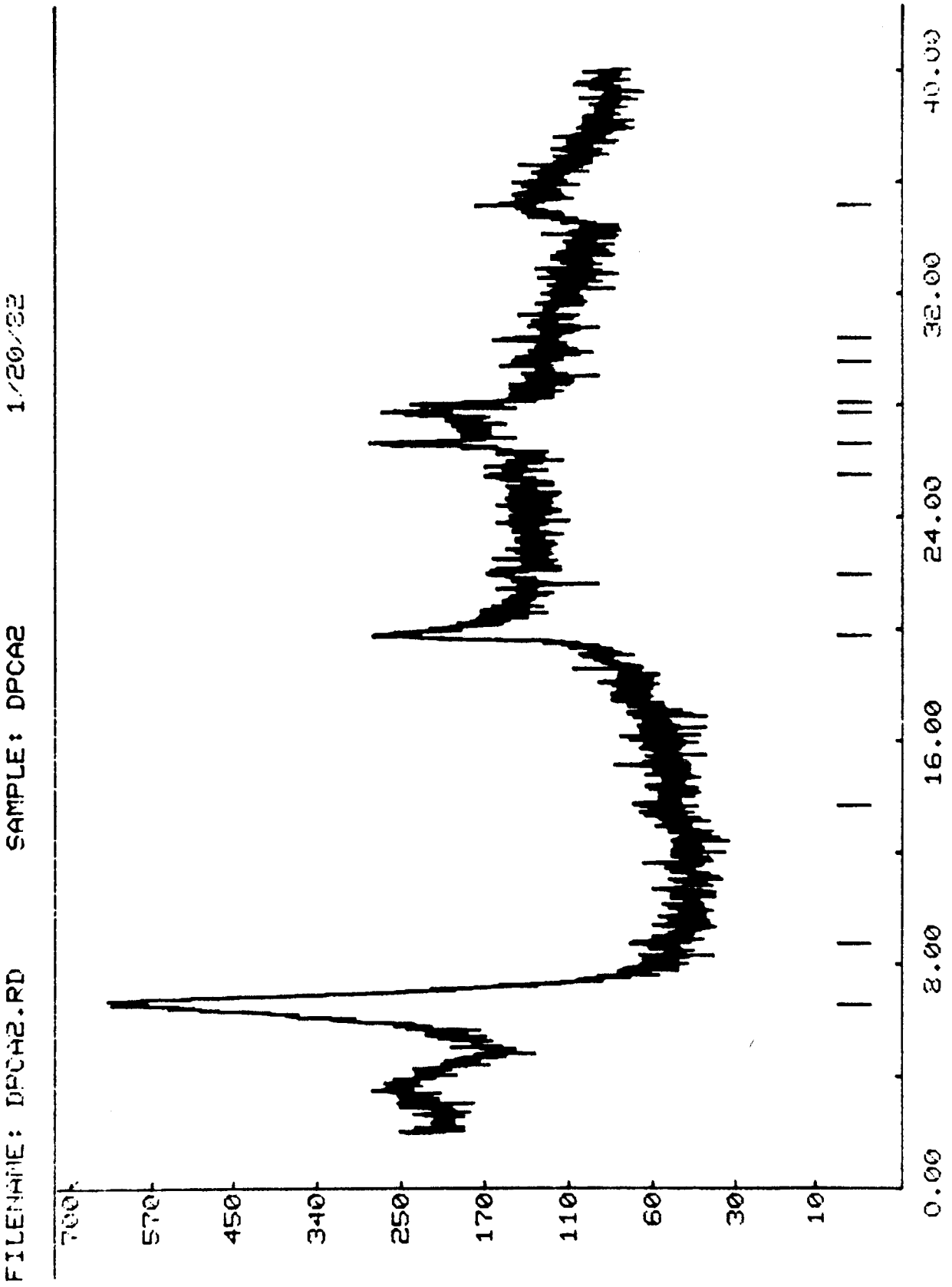

Fig. 6b. X-ray diffractogram for 0.5 mm distance from the copper/bentonite interface.

APD-3600 2ND DERIVATIVE PEAK ALGORITHM 1/20/82 13:45:51

RAW DATA FILE : DPCA3.RD
SAMPLE ID : DPCA3
RAW DATA FILE DATE : 1/19/82
GENERATOR SETTINGS : 40 KV 30 MA
STEP SIZE, CNT TIME : 0.020 DEG 0.50 SEC
RANGE OF DATA : 2.000 - 65.000 DEG
RANGE IN D : 44.1372 - 1.4337 A
MAX PEAK CTS, CPS : 380. CTS 760. CPS
SECF APPLIED : NONE

2-THETA (DEG)	WIDTH (APPROX)	COUNTS PEAK	COUNTS BKGND	D (ANG)	I (NORM)	LINE TYPE a1	LINE TYPE a2	LINE TYPE BT	LINE TYPE AM	LINE TYPE OT
3.77	0.38	49.	166.	23.3870	12.89	X	X			
6.83	0.77	380.	86.	12.9315	100.00	X	X			
8.81	0.34	27.	49.	10.0292	7.11	X	X			
9.96	0.30	10.	42.	8.8736	2.53	X	X			
14.12	0.00	18.	55.	6.2650	4.86	U	U			
19.81	0.18	182.	92.	4.4781	47.93	X	X			
20.76	0.00	69.	106.	4.2743	18.12	U	U			
21.97	0.29	56.	121.	4.0425	14.79	X	X			
26.62	0.25	132.	137.	3.3459	34.78	X	X			
27.43	0.14	106.	135.	3.2495	27.90	X	X			
27.71	0.20	161.	132.	3.2167	42.42	X	X			
28.05	0.19	130.	132.	3.1785	34.18	X	X			
29.52	0.25	18.	128.	3.0235	4.86	X	X			
29.96	0.13	49.	128.	2.9801	12.89	X	X			
35.12	0.00	31.	119.	2.5532	8.25	U	U			
36.68	0.00	7.	112.	2.4484	1.78	U	U			
48.49	0.30	13.	77.	1.8760	3.41	X	X			
54.25	0.00	27.	85.	1.6895	7.11	U	U			
61.96	0.47	46.	88.	1.4964	12.16	X	X			

19 PEAKS IDENTIFIED 19 CRYSTALLINE 0 AMORPHOUS
19 PEAKS LISTED

Fig. 7a. Recorded X-ray data for 1.0 mm distance from the copper/bentonite interface.

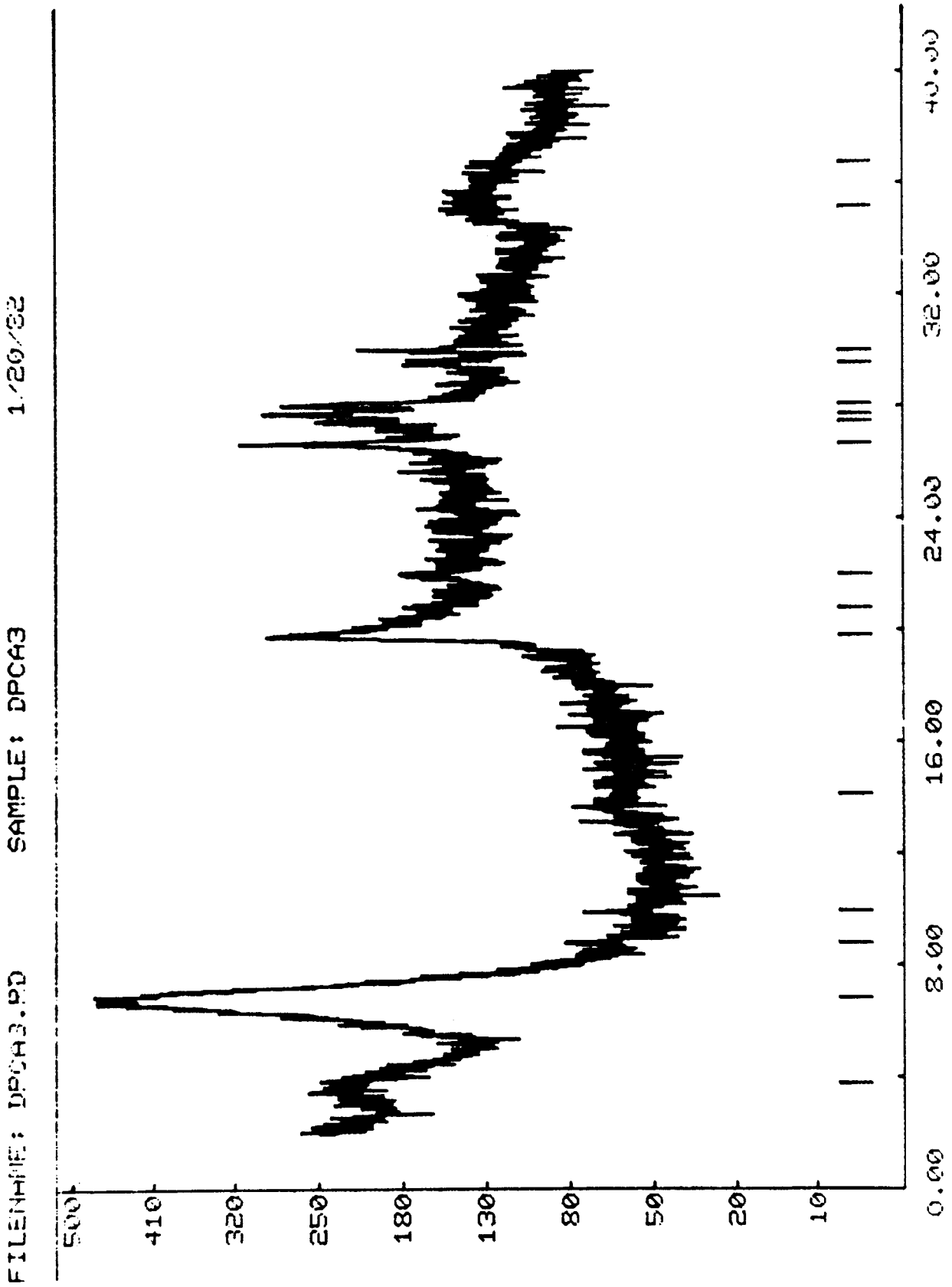

Fig. 7b. X-ray diffractogram for 1.0 mm distance from the copper/bentonite interface.

APD-3600 2ND DERIVATIVE PEAK ALGORITHM 1/20/82 13:46:36

RAW DATA FILE : DPCA4.RD
SAMPLE ID : DPCA4
RAW DATA FILE DATE : 1/19/82
GENERATOR SETTINGS : 40 KV 30 MA
STEP SIZE, CNT TIME : 0.020 DEG 0.50 SEC
RANGE OF DATA : 2.000 - 65.000 DEG
RANGE IN D : 44.1372 - 1.4337 A
MAX PEAK CTS, CPS : 324. CTS 648. CPS
SECF APPLIED : NONE

2-THETA (DEG)	WIDTH (APPROX)	COUNTS PEAK	COUNTS BKGND	D (ANG)	I (NORM)	LINE TYPE a1	LINE TYPE a2	LINE TYPE BT	LINE TYPE AM	LINE TYPE OT
4.17	0.00	48.	166.	21.1725	14.69	U	U			
6.90	0.18	324.	114.	12.8005	100.00	X	X			
8.73	0.00	19.	66.	10.1151	5.98	U	U			
13.74	0.00	20.	50.	6.4374	6.25	U	U			
19.77	0.26	182.	85.	4.4859	56.25	X	X			
20.76	0.00	77.	94.	4.2743	23.90	U	U			
22.01	0.40	52.	106.	4.0343	16.00	X	X			
23.57	0.38	42.	121.	3.7708	13.04	X	X			
24.45	0.00	32.	128.	3.6378	10.03	U	U			
26.62	0.29	128.	135.	3.3466	39.41	X	X			
27.66	0.12	108.	135.	3.2219	33.38	X	X			
28.06	0.20	56.	135.	3.1774	17.36	X	X			
29.54	0.00	40.	128.	3.0220	12.25	U	U			
34.93	0.46	40.	104.	2.5666	12.25	X	X			
36.45	0.00	25.	106.	2.4630	7.72	U	U			
41.62	0.31	12.	88.	2.1682	3.57	X	X			
47.43	0.00	19.	79.	1.9153	5.98	U	U			
48.57	0.27	13.	77.	1.8730	4.00	X	X			
54.44	0.00	23.	85.	1.6841	7.11	U	U			
61.94	0.50	32.	86.	1.4969	10.03	X	X			

Fig. 8a. Recorded X-ray data for 2.0 mm distance from the copper/bentonite interface.

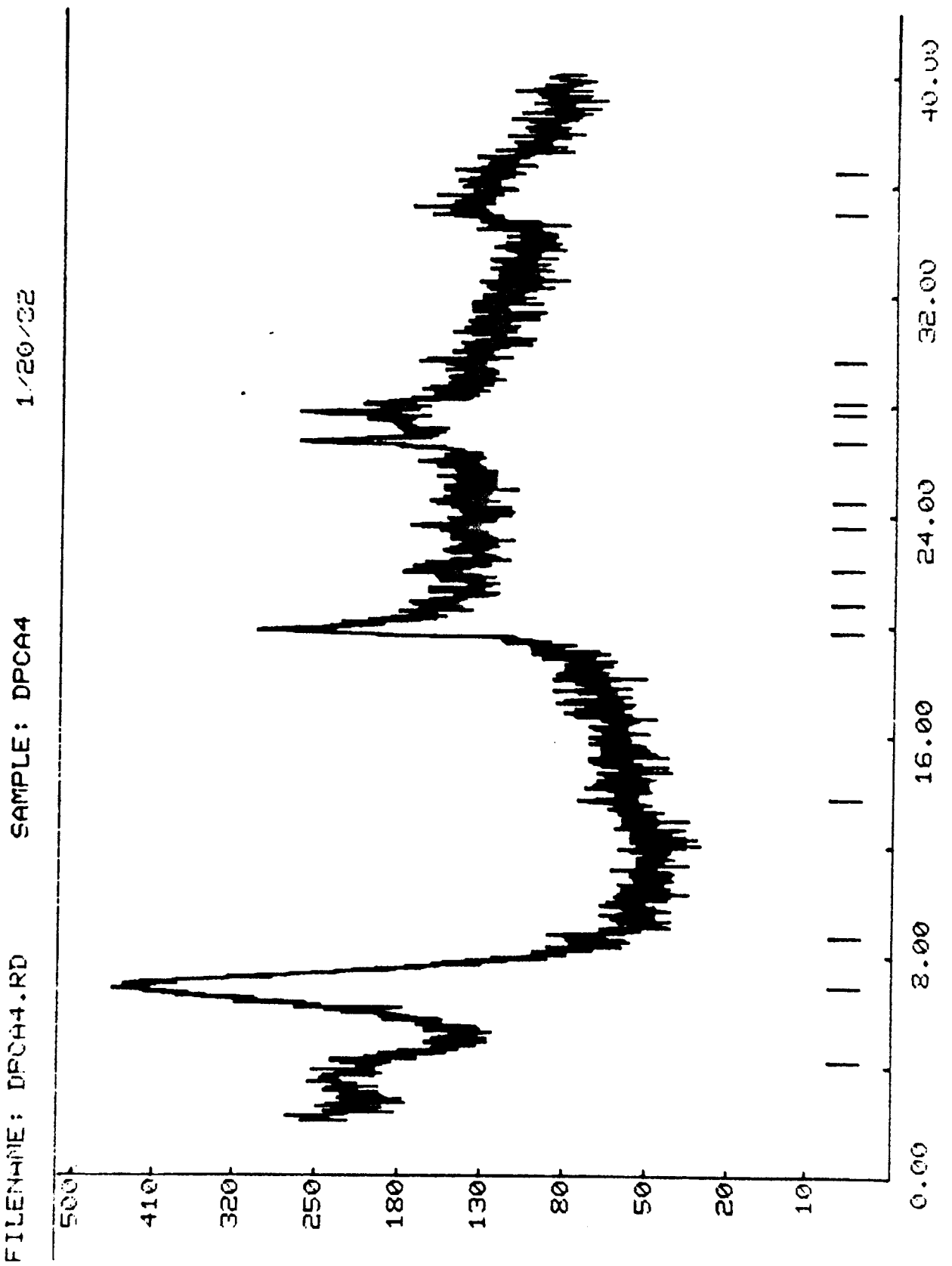

Fig. 8b. X-ray diffractogram for 2.0 mm distance from the copper/bentonite interface.

the Cu concentration is approximately constant within the 0-2 mm interval from the copper/bentonite interface, indicating that Cu has not migrated extensively from the solid Cu body into the clay. The recorded, very low Cu content of the clay distant from the copper plate obviously originates from accessory minerals, organics, or sea water which were all present when the clay was formed in nature.

Case II

The second test was run as part of a borehole sealing experiment (cf. PUSCH, 1981) in which a perforated copper pipe was inserted in a ø 38 mm borehole in the Stripa mine, the pipe being filled with ø 30 mm highly compacted Na bentonite cylinders. The outer and inner diameters of the pipe, which was perforated to about 50% of its surface area, was 35 and 32 mm, respectively. The bentonite plug sealing was left in the hole for six months after which the hole was overcored. The rock core was cut, perpendicularly to the long axis, yielding 50 mm thick discs with an outer diameter of 143 mm, their central part being the clay plug (Fig. 9). One of the discs was used for axial percolation to determine the permeability of the plug, which had become fairly homogeneous with a bulk density of about 1.8 t/m^3 and a water content of approximately 42% of the clay just inside the pipe. This plug was extruded after the percolation test to determine the "bond strength", i.e. the maximum shear strength at the interface rock/clay. The plug was then cut open to yield a cylindrical clay sample, the outer boundary of which was the interface copper/bentonite. This interface was lustreless and cinnabar-colored, indicating a coating of copper Ioxide. The plug was used for analysis of the bentonite with respect to X-ray diffraction characteristics and to element distributions in the same way as described for Case I.

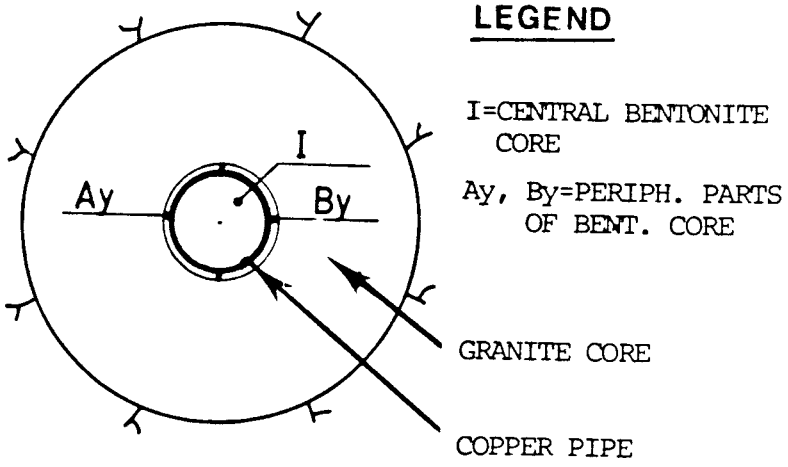

Fig. 9. Schematic section through rock core with central clay plug.

Results

* The X-ray diffractograms (see Fig. 10-13) show the same general pattern as in Case I, although Case 2 exhibits stronger variations in peak height and width and thus in mineral composition. At least at the interface of the copper/bentonite certain peaks – unidentified so far with respect to the origin – may be related to the formation of copper components. It is clear, however, that the (001) reflexions are not affected by the proximity of the copper as it was in Case 1. In the present case we find the D-value to be in the interval 12.61-12.86 Å for all the investigated specimens; hence, there is no indication of Na being replaced by Cu.

APD-3600 2ND DERIVATIVE PEAK ALGORITHM 1/20/82 13:40:32

RAW DATA FILE : DPCR1.RD = Cu RADIAL INTERFACE
SAMPLE ID : DPCR1
RAW DATA FILE DATE : 1/19/82
GENERATOR SETTINGS : 40 KV 30 MA
STEP SIZE, CNT TIME : 0.020 DEG 0.50 SEC
RANGE OF DATA : 2.000 - 65.000 DEG
RANGE IN D : 44.1372 - 1.4337 A
MAX PEAK CTS, CPS : 388. CTS 776. CPS
SECF APPLIED : NONE

2-THETA (DEG)	WIDTH (APPROX)	COUNTS PEAK	COUNTS BKGND	D (ANG)	I (NORM)	LINE TYPE a1	LINE TYPE a2	LINE TYPE BT	LINE TYPE AM	LINE TYPE OT
6.87	0.83	388.	104.	12.8563	100.00	X	X			
8.78	0.00	11.	76.	10.0634	2.81	U	U			
11.63	0.27	53.	56.	7.6029	13.73	X	X			
13.70	0.00	18.	62.	6.4561	4.76	U	U			
15.08	0.00	24.	66.	5.8704	6.19	U	U			
19.83	0.37	108.	108.	4.4736	27.87	X	X			
20.82	0.20	62.	125.	4.2631	16.08	X	X			
21.95	0.00	36.	139.	4.0461	9.23	U	U			
23.41	0.00	31.	144.	3.7962	8.08	U	U			
26.65	0.30	96.	142.	3.3429	24.75	X	X			
27.34	0.00	77.	142.	3.2600	19.95	U	U			
27.71	0.50	132.	139.	3.2162	34.08	X	X			
28.05	0.19	66.	139.	3.1780	16.91	X	X			
29.17	0.33	50.	137.	3.0590	12.99	X	X			
29.88	0.00	27.	135.	2.9874	6.97	U	U			
31.22	0.00	28.	130.	2.8626	7.24	U	U			
34.73	0.00	23.	119.	2.5813	5.94	U	U			
36.45	0.38	67.	112.	2.4633	17.33	X	X			
43.38	0.39	12.	96.	2.0840	3.16	X	X			
47.98	0.00	21.	85.	1.8946	5.45	U	U			

Fig. 10a. Recorded X-ray data for the copper/bentonite interface.

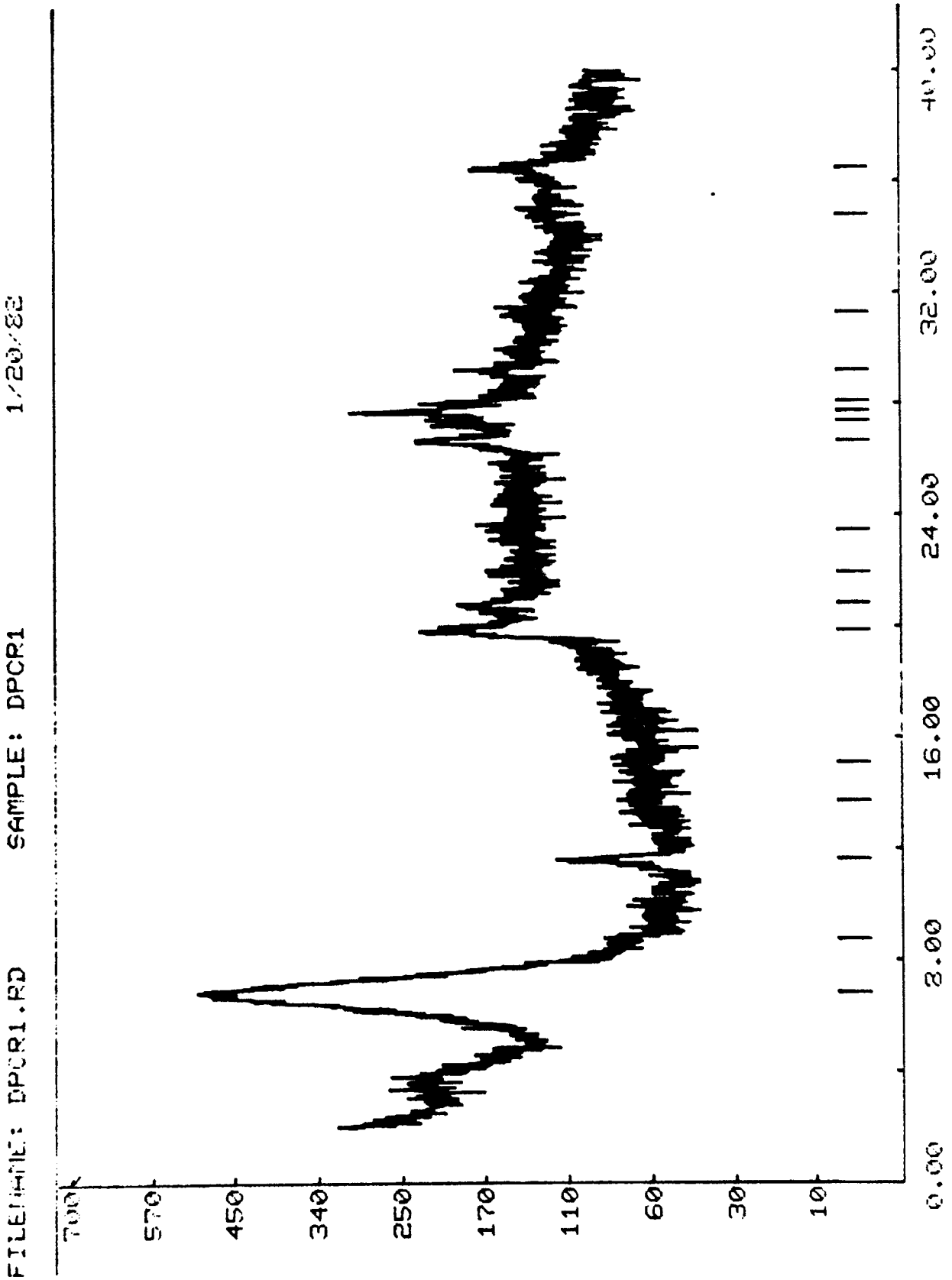

Fig. 10b. X-ray diffractogram for the copper/bentonite interface.

APD-3600 2ND DERIVATIVE PEAK ALGORITHM 1/20/82 13:39:57

RAW DATA FILE	:	DPCR2.RD
SAMPLE ID	:	DPCR2
RAW DATA FILE DATE	:	1/19/82
GENERATOR SETTINGS	:	40 KV 30 MA
STEP SIZE, CNT TIME	:	0.020 DEG 0.50 SEC
RANGE OF DATA	:	2.000 - 65.000 DEG
RANGE IN D	:	44.1372 - 1.4337 A
MAX PEAK CTS, CPS	:	296. CTS 592. CPS
SECF APPLIED	:	NONE

2-THETA (DEG)	WIDTH (APPROX)	COUNTS PEAK	COUNTS BKGND	D (ANG)	I (NORM)	LINE TYPE a1	LINE TYPE a2	LINE TYPE BT	LINE TYPE AM	LINE TYPE OT
7.01	0.64	296.	88.	12.6088	100.00	X	X			
8.69	0.00	26.	64.	10.1674	8.79	U	U			
14.19	0.00	20.	56.	6.2365	6.84	U	U			
19.80	0.39	135.	106.	4.4792	45.48	X	X			
20.57	0.00	46.	121.	4.3143	15.63	U	U			
22.02	0.11	276.	137.	4.0334	93.15	X	X			
24.30	0.00	23.	139.	3.6599	7.79	U	U			
26.64	0.21	121.	144.	3.3435	40.90	X	X			
27.34	0.00	56.	144.	3.2600	19.01	U	U			
27.70	0.20	106.	144.	3.2179	35.86	X	X			
28.05	0.18	72.	144.	3.1780	24.42	X	X			
34.90	0.27	20.	112.	2.5691	6.84	X	X			
61.99	0.33	18.	90.	1.4959	5.96	X	X			

13 PEAKS IDENTIFIED 13 CRYSTALLINE 0 AMORPHOUS

13 PEAKS LISTED

Fig. 11a. X-ray data for 0.5 mm distance from the copper/bentonite interface.

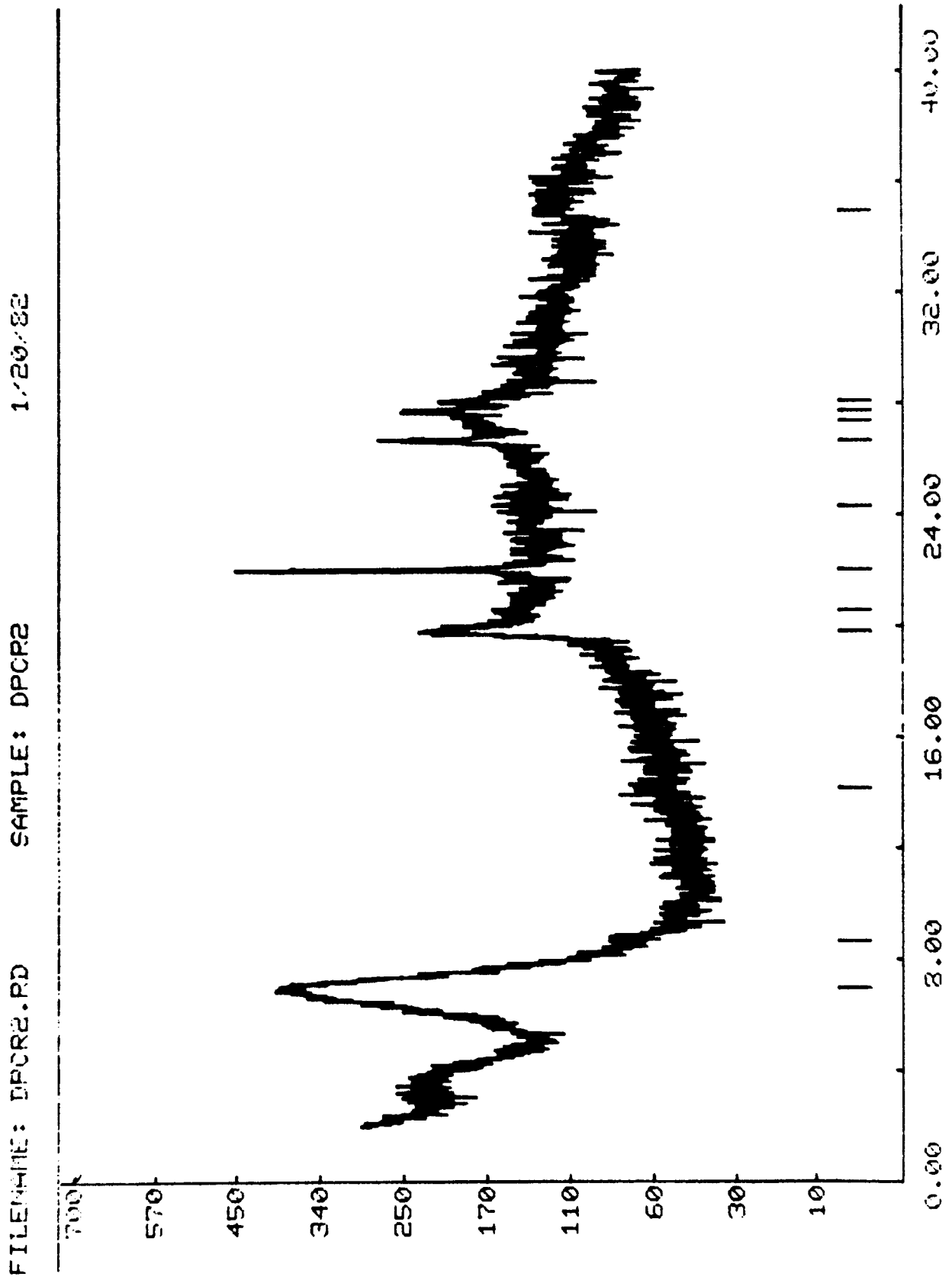

Fig. 11b. X-ray diffractogram for 0.5 mm distance from the interface.

APD-3600 2ND DERIVATIVE PEAK ALGORITHM 1/20/82 13:39:30

RAW DATA FILE : DPCR3.RD
SAMPLE ID : DPCR3
RAW DATA FILE DATE : 1/19/82
GENERATOR SETTINGS : 40 KV 30 MA
STEP SIZE, CNT TIME : 0.020 DEG 0.50 SEC
RANGE OF DATA : 2.000 - 65.000 DEG
RANGE IN D : 44.1372 - 1.4337 A
MAX PEAK CTS, CPS : 320. CTS 641. CPS
SECF APPLIED : NONE

2-THETA (DEG)	WIDTH (APPROX)	COUNTS PEAK	COUNTS BKGND	D (ANG)	I (NORM)	LINE TYPE a1	LINE TYPE a2	LINE TYPE BT	LINE TYPE AM	LINE TYPE OT
6.93	0.75	320.	94.	12.7543	100.00	X	X			
8.65	0.00	11.	67.	10.2202	3.40	U	U			
13.92	0.00	27.	53.	6.3546	8.44	U	U			
19.80	0.32	112.	110.	4.4792	35.07	X	X			
20.80	0.00	38.	132.	4.2671	12.00	U	U			
21.92	0.33	14.	142.	4.0516	4.51	X	X			
23.68	0.00	18.	142.	3.7551	5.51	U	U			
26.62	0.23	90.	146.	3.3466	28.17	X	X			
27.70	0.16	142.	151.	3.2185	44.20	X	X			
28.01	0.14	114.	151.	3.1835	35.73	X	X			
29.48	0.37	19.	142.	3.0280	6.04	X	X			
34.99	0.00	36.	114.	2.5623	11.24	U	U			
35.92	0.00	19.	114.	2.4981	6.04	U	U			
41.62	0.31	18.	86.	2.1682	5.51	X	X			
54.24	0.00	21.	86.	1.6896	6.60	U	U			
61.88	0.33	26.	88.	1.4983	8.12	X	X			
62.37	0.00	25.	88.	1.4877	7.80	U	U			

17 PEAKS IDENTIFIED 17 CRYSTALLINE 0 AMORPHOUS
17 PEAKS LISTED

Fig. 12a. X-ray data for 1.0 mm distance from the copper/bentonite interface.

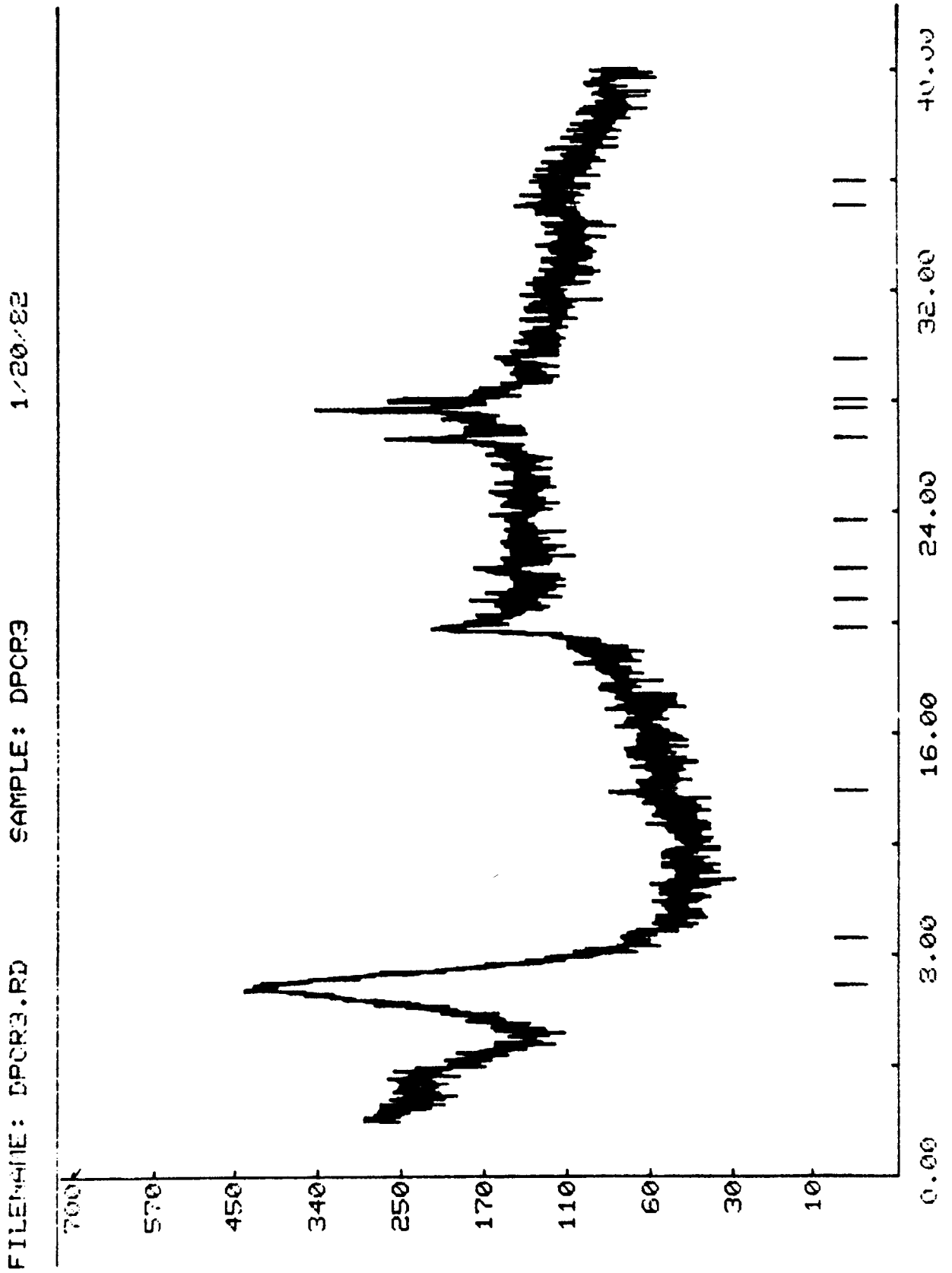

Fig. 12b. X-ray diffractogram for 1.0 mm distance from the copper/bentonite interface.

APD-3600 2ND DERIVATIVE PEAK ALGORITHM 1/20/82 13:38:40

RAW DATA FILE : DPCR4.RD
SAMPLE ID : DPCR4
RAW DATA FILE DATE : 1/19/82
GENERATOR SETTINGS : 40 KV 30 MA
STEP SIZE, CNT TIME : 0.020 DEG 0.50 SEC
RANGE OF DATA : 2.000 - 65.000 DEG
RANGE IN D : 44.1372 - 1.4337 A
MAX PEAK CTS, CPS : 331. CTS 662. CPS
SECF APPLIED : NONE

2-THETA (DEG)	WIDTH (APPROX)	COUNTS PEAK	COUNTS BKGND	D (ANG)	I (NORM)	LINE TYPE a1	LINE TYPE a2	LINE TYPE BT	LINE TYPE AM	LINE TYPE OT
3.72	0.49	66.	174.	23.7646	19.81	X	X			
6.92	0.73	266.	28.	12.7635	80.21	X	X			
13.67	0.35	7.	50.	6.4725	2.20	X	X			
19.80	0.32	180.	90.	4.4792	54.21	X	X			
20.80	0.00	74.	104.	4.2671	22.33	U	U			
21.96	0.33	35.	121.	4.0443	10.51	X	X			
23.60	0.25	35.	135.	3.7660	10.51	X	X			
26.66	0.15	331.	149.	3.3404	100.00	X	X			
27.70	0.25	121.	149.	3.2179	36.53	X	X			
28.02	0.12	67.	146.	3.1819	20.30	X	X			
29.49	0.31	34.	132.	3.0270	10.16	X	X			
34.88	0.50	28.	104.	2.5698	8.48	X	X			
54.85	0.00	24.	86.	1.6723	7.25	U	U			
61.99	0.38	35.	86.	1.4957	10.51	X	X			

14 PEAKS IDENTIFIED 14 CRYSTALLINE 0 AMORPHOUS
14 PEAKS LISTED

Fig. 13a. X-ray data for 2.0 mm distance from the copper/bentonite interface.

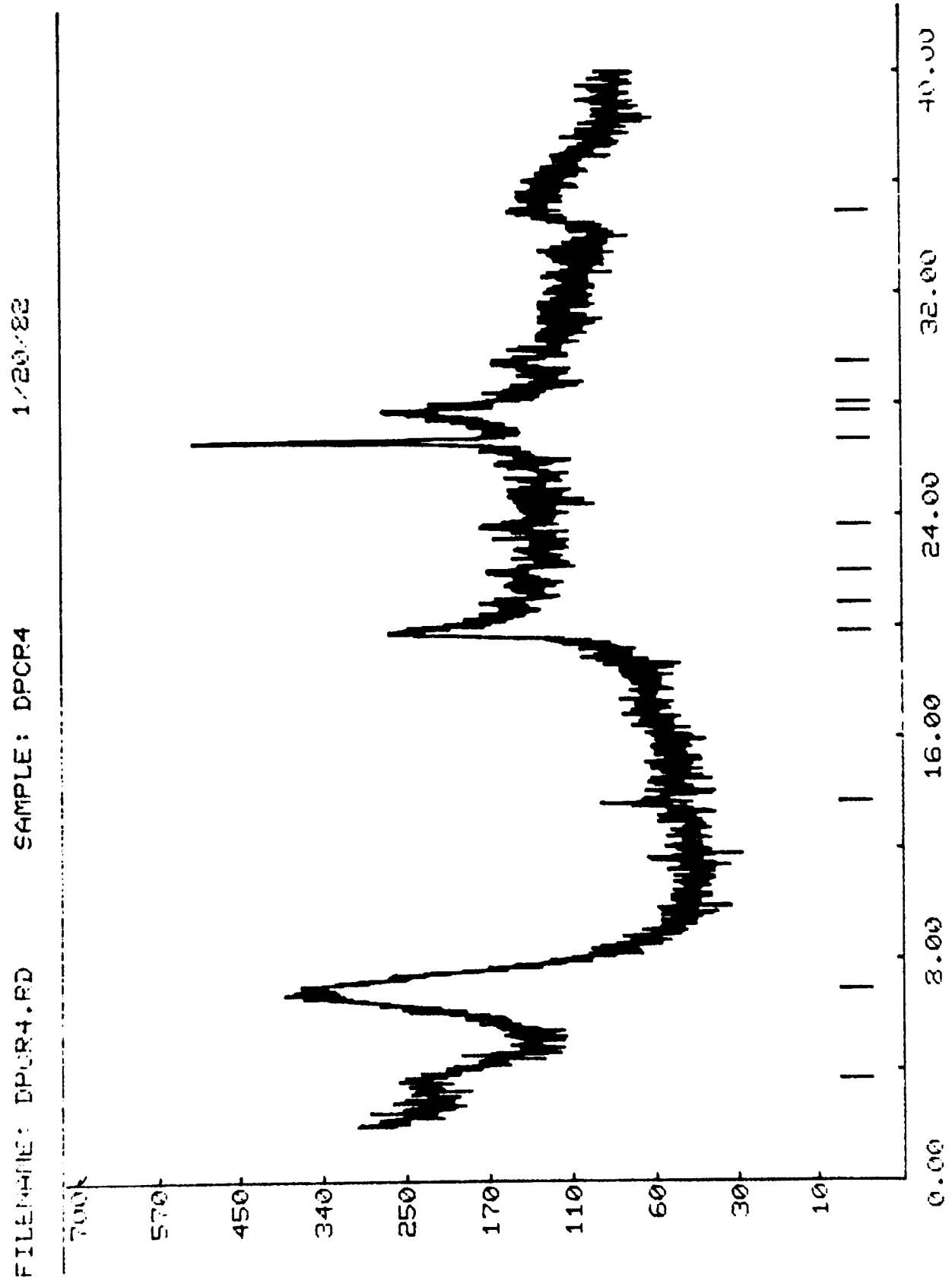

Fig. 13b. X-ray diffractogram for 2.0 mm distance from the copper/bentonite interface.

* The element analyses have been interpreted as follows (cf. Appendix 2).

a) The two copper line scans (Plate 10 and 11) show a higher Cu concentration in the first 0.5 mm distance from the copper/bentonite interface than the average Cu content in the clay. Notice that Plate 10 exhibits detector saturation to within about 0.3 mm from the interface; Plate 12 shows the result of a repeated scanning at reduced sensitivity. Here we find a very high Cu concentration at the interface, its origin being the red coating.

b) The full area copper maps show the same pattern as the line scans; i.e. a very high frequency of bright spots at the copper/ /bentonite interface with a drop in frequency to within about 0.5 mm distance from the interface. At larger distances we find a fairly uniform distribution of a small number of very faint spots indicating no Cu concentration gradient.

c) The examination of the micrographs showed the typical microstructural features of Na montmorillonite. The micrographs of the interface also illustrate the "red coating", which contains montmorillonite as well as copper compounds. Plates 13-19 indicate the presence of Si, Al, Fe, Ca, Cu, and S, the relative peak height of copper being of primary interest. The expected high Cu concentration at the copper/bentonite interface is verified by Plate 13, and at

larger distances we find the successive Cu concentration that is expected from the "line" and "full area" scans.

Discussion and conclusions

Theoretical considerations suggest that ionic migration of copper should be very limited and slow in the pH-range of sodium bentonite. Two experiments support this conclusion although they yield different bentonite/copper interaction scenarios. A "Sandwich" test, in which the contact between bentonite and copper was intimate already at the start of the water uptake in the bentonite, did not allow for any extensive copper oxidation or hydroxylation. Hence, copper essentially being metallic, was contacted with water-rich bentonite throughout the test. This yielded fairly comprehensive copper ion migration into the adjacent clay where sodium ions tended to be replaced by copper ions. This is a true ion exchange phenomenon which only affects the electrical intra-aggregate force fields without having any cementing effect. It is possible, or even probable, that direct contact between the central steel axis and the copper disc produced electrical potentials which were largely responsible for the dissolution of the copper[1)].

The "borehole" test resembles the conditions in a deposition hole much more. Thus, there is a slot between the metallic copper and the bentonite and this slot is slowly filled by bentonite expanding from the central part in the course of the water uptake. The copper/bentonite interface was rich in entrapped air and various copper compounds were consequently formed ("the red coating") before any tight contact was established with the expanding bentonite. The boundary zone, where these compounds were formed and which was invaded by initially very soft, expanding clay, must have been 0.5-1 mm wide in the experiment. The absence of observable ion exchange (from Na to Cu) suggests that the copper present in the bentonite is actually copper compounds of low solubility, intermingled with the bentonite. It is therefore not relevant to deduce any real or pseudo-diffusion

---

1) Pers. comm. Prof. Ingemar Grenthe, Dep. Chem. KTH, Sweden.

coefficient of ionic copper migration in bentonite on the basis of the present data.

Although ionic Cu migration can be estimated to be extremely slow as concluded from the present study, it may well migrate into the clay in sufficient amounts to produce ion exchange and certain clay particle rearrangement in the entire bentonite envelope during the lifetime of a KBS 2 canister. As mentioned previously in the text, this has but one important bearing on the physical properties of the bentonite: the permeability will probably be increased by about 2 to 5 times. Considering the extremely low permeability of the highly compacted Na bentonite, i.e. about 10^{-13} m/s at 100% water saturation, we find, however, the influence on the permeability to be of insignificant importance.

References

CLEMENTZ, D. M., MORTLAND, M.M. & PINNAVAIA, T.J., 1974. Properties of reduced charge montmorillonites: Hydrated Cu (II) ions as a spectroscopic probe. Clays and Clay Minerals, Vol. 22., Pergamon Press (G.B.), pp. 49-57.

KRAUSKOPF; K.B., 1967. Introduction to geochemistry. McGraw-Hill Book Company, New York, Int. Series in the earth and planetary sciences.

PUSCH, R., 1981. Borehole sealing with highly compacted Na bentonite. KBS Technical Report 81-09.

PUSCH, R., 1982. Mineral/water interactions and their influence on the physical behavior of highly compacted Na bentonite. Can. Geot. J. 1982 (In press).

APPENDIX 1

ELEMENT ANALYSES (EMV)

PLATES 1-9

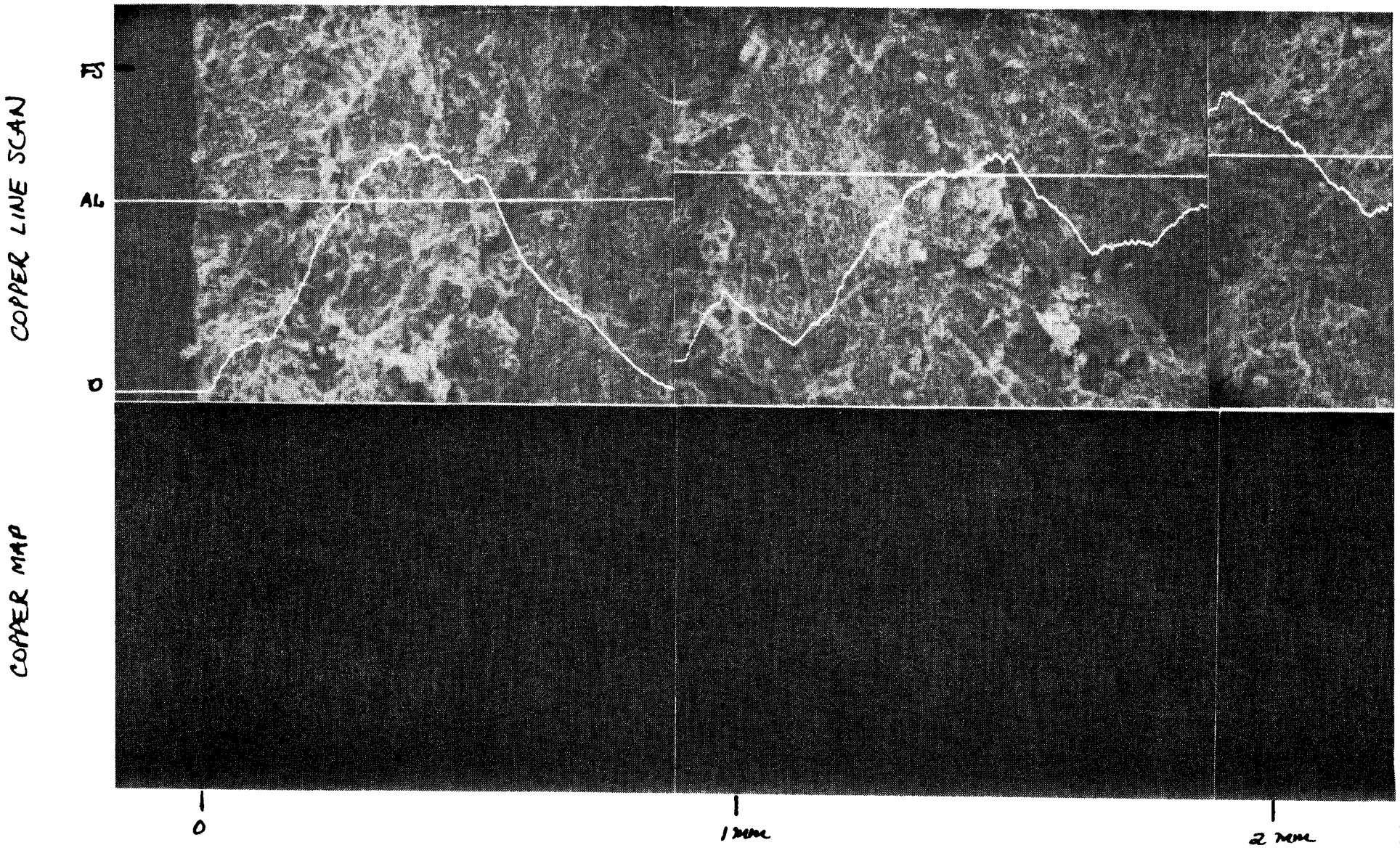

PLATE 1

SAMPLE: C-Q
RUN: 1

LINE ANALYSIS
FS SENSITIVITY: 0.5×10^2 CPS
SCAN SETTING: 6

AL ≡ ANALYSIS LINE
FS ≡ FULL SCALE
CPS ≡ COUNTS PER SECOND

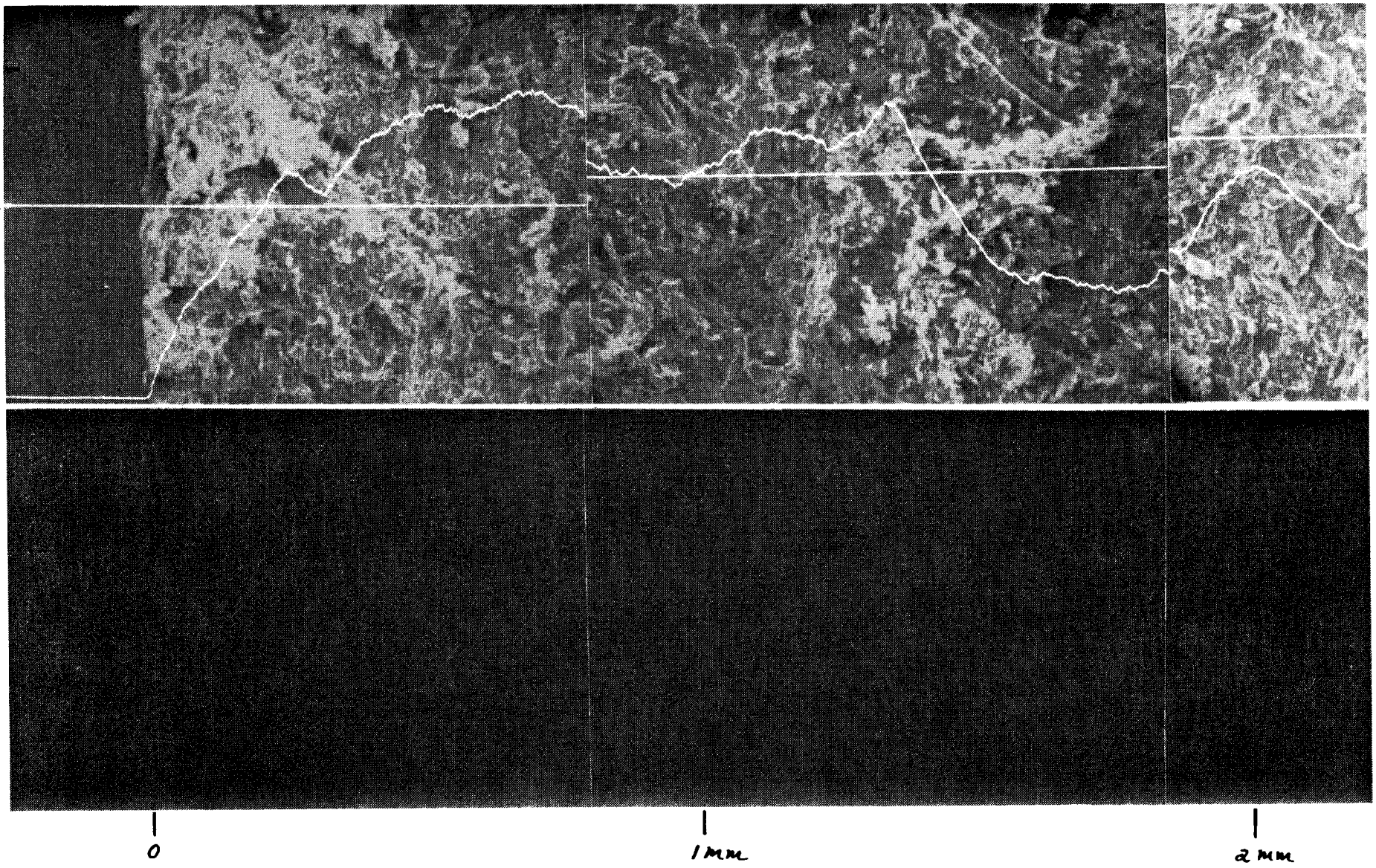

SAMPLE: C-a
RUN: 2

LINE ANALYSIS
FS SENSITIVITY: 0.5×10^2 CPS
SCAN SETTING: 6

AL ≡ ANALYSIS LINE
FS ≡ FULL SCALE
CPS ≡ COUNTS PER SECOND

PLATE 2

PLATE 3

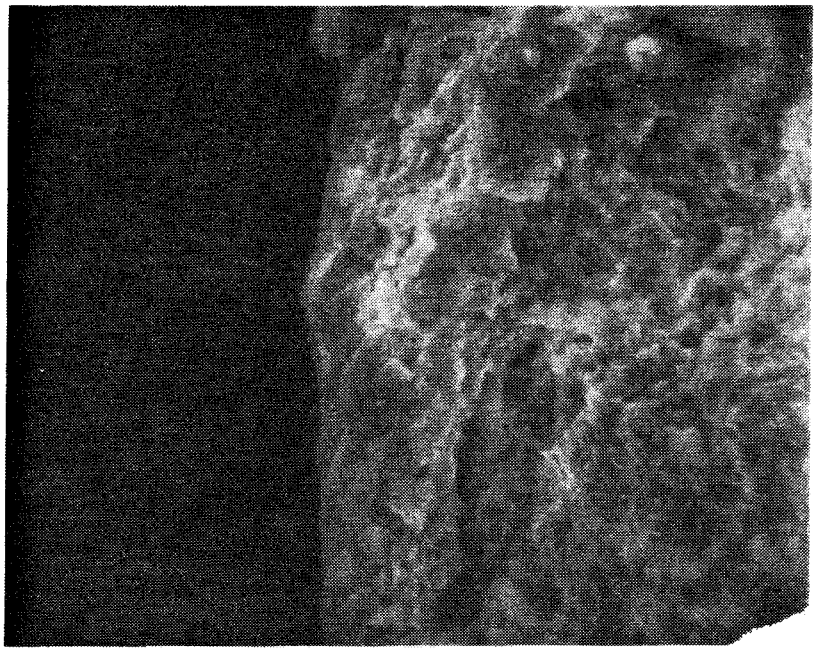

500 X

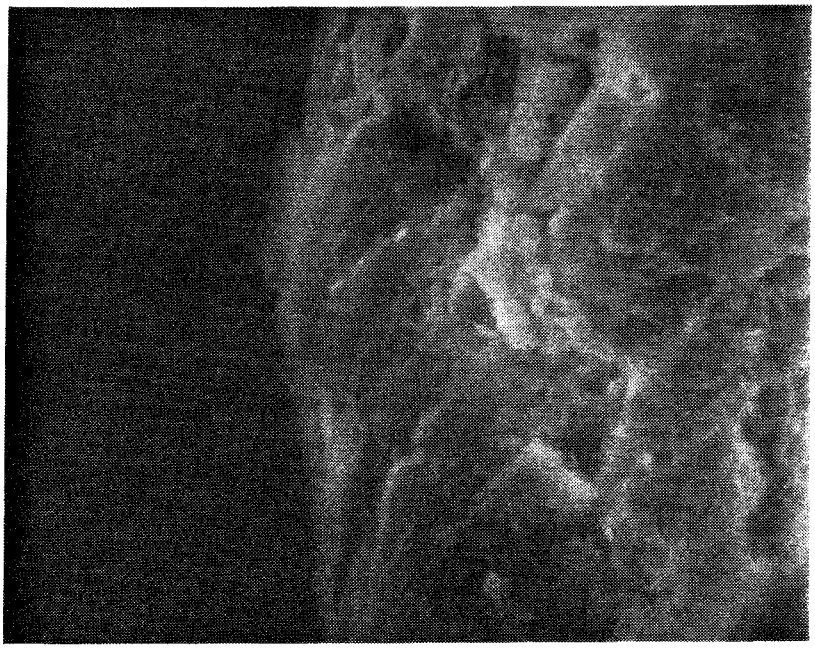

1500 X

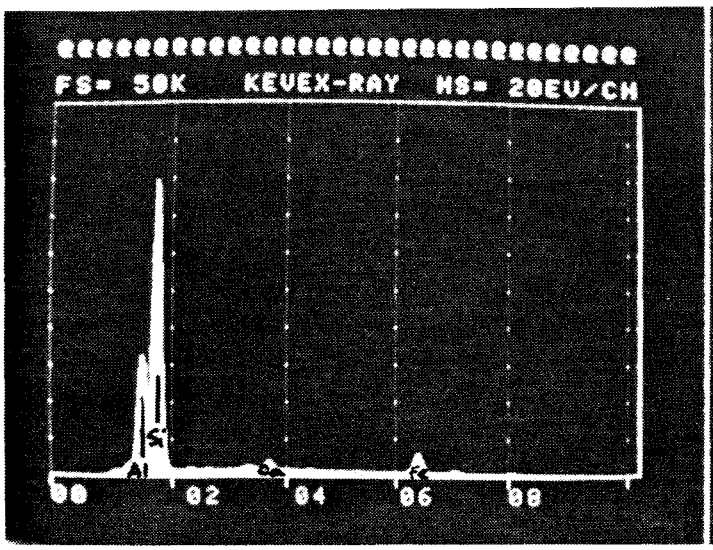

SMALL AREA SCAN @ 1500 X

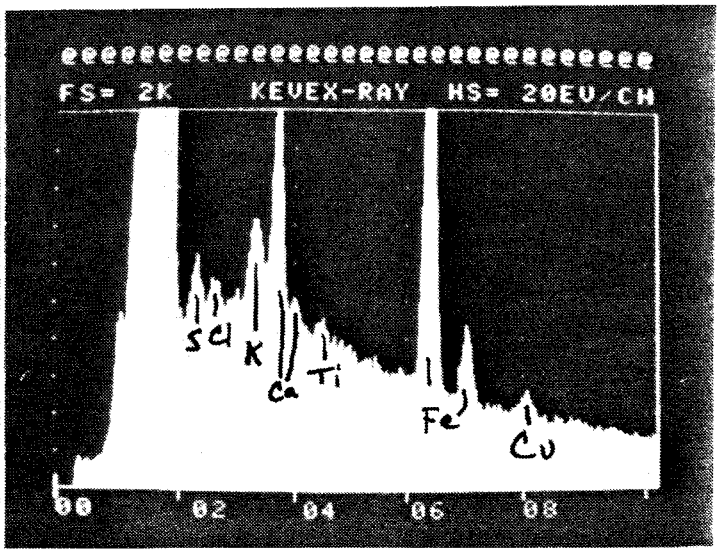

EXPANDED SCALE

SAMPLE: C-a
RUN: 2

POSITION: AT INTERFACE

PLATE 4

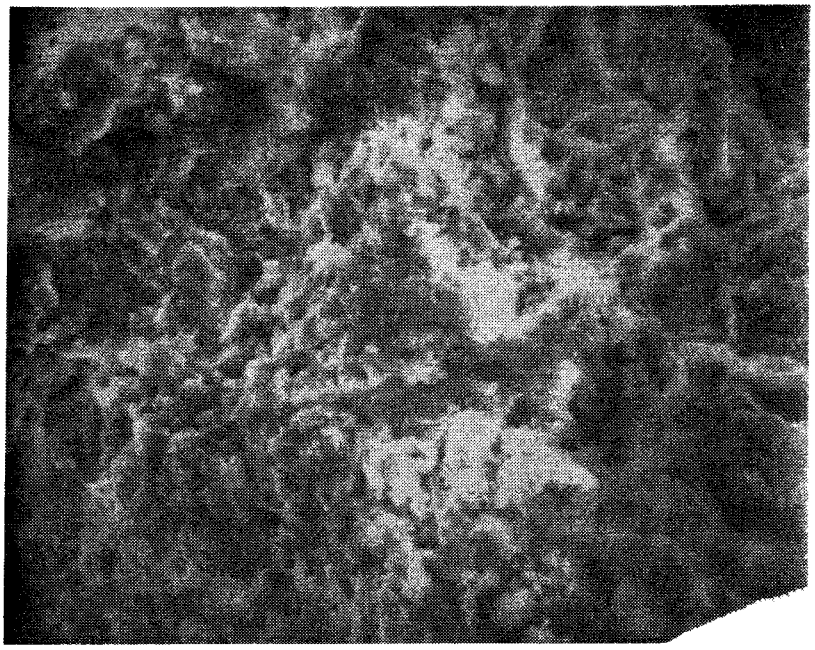

500 X

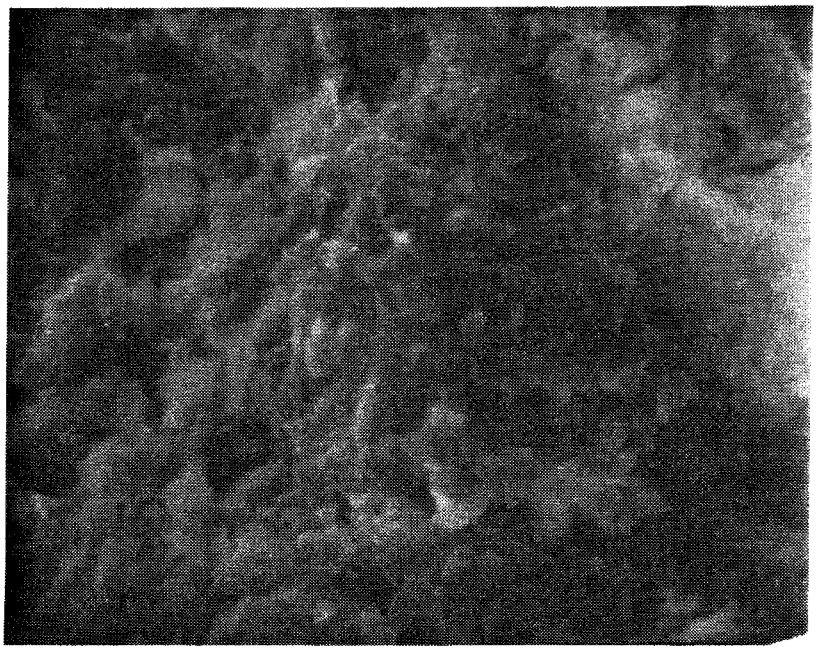

1500 X

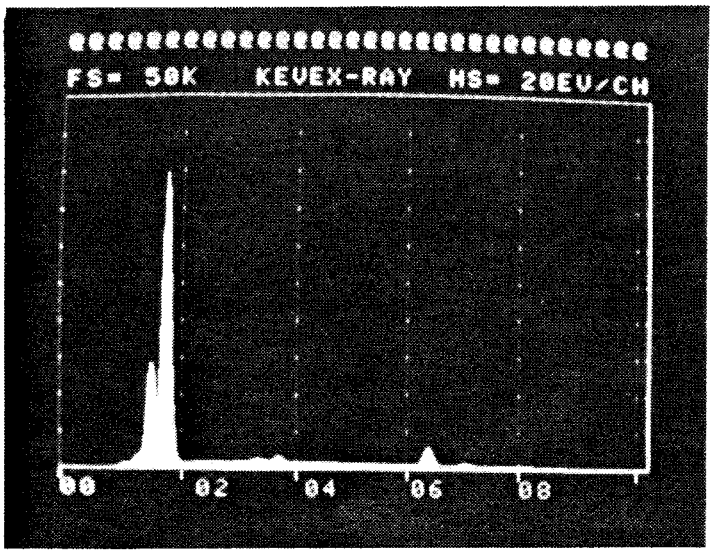

SMALL AREA SCAN @ 1500 X

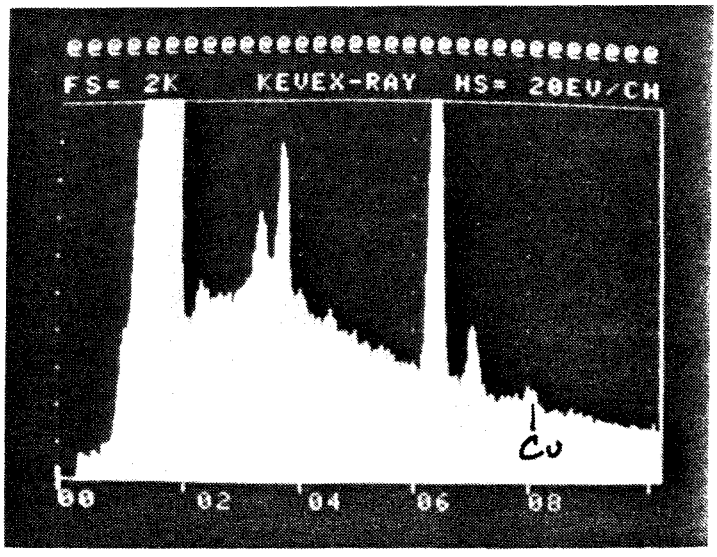

EXPANDED SCALE

SAMPLE: C-a
RUN: 2

POSITION: 0.1 mm

PLATE 5

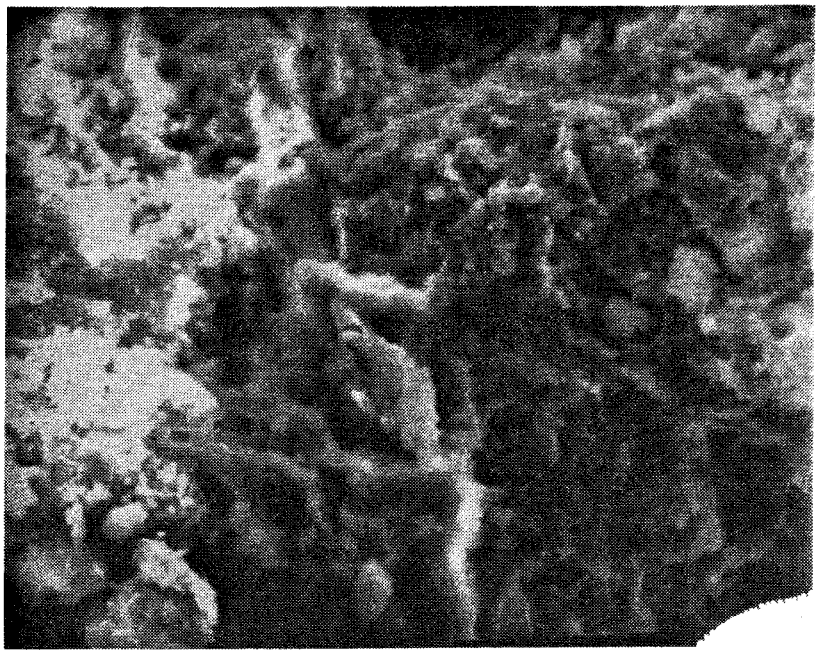

500 X

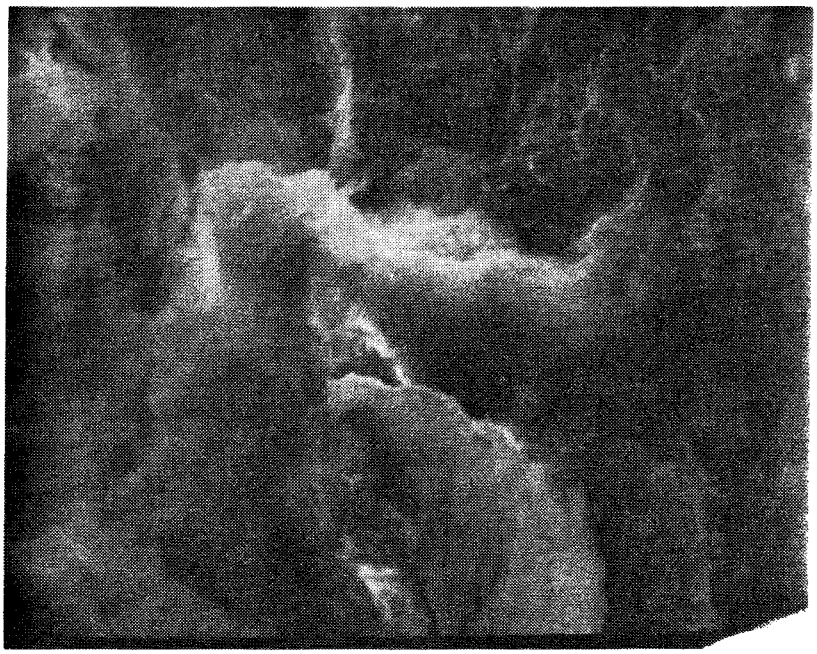

1500 X

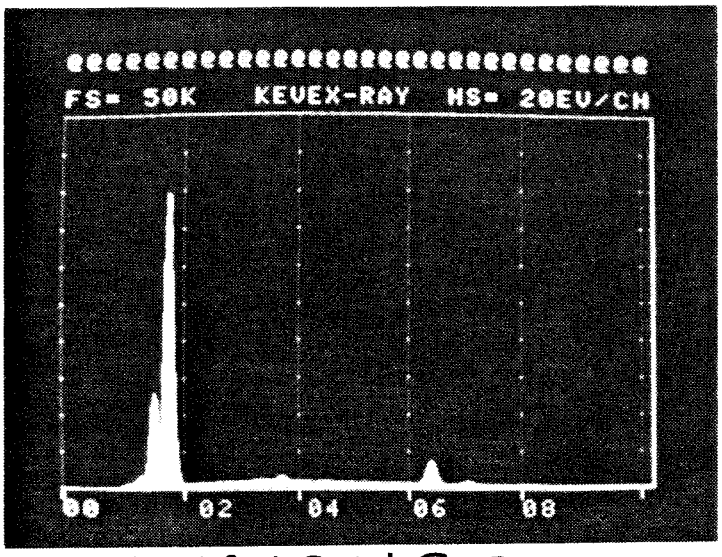

SMALL AREA SCAN @ 1500 X

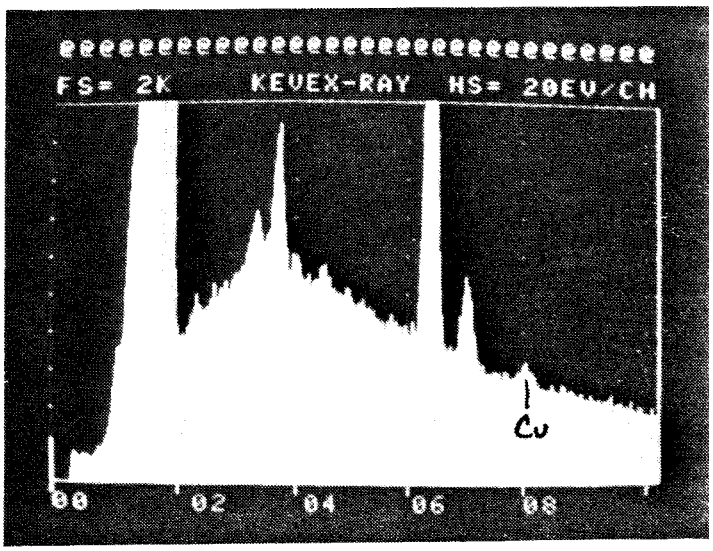

EXPANDED SCALE

SAMPLE: C-a
RUN: 2

POSITION: 0.2 mm

PLATE 6

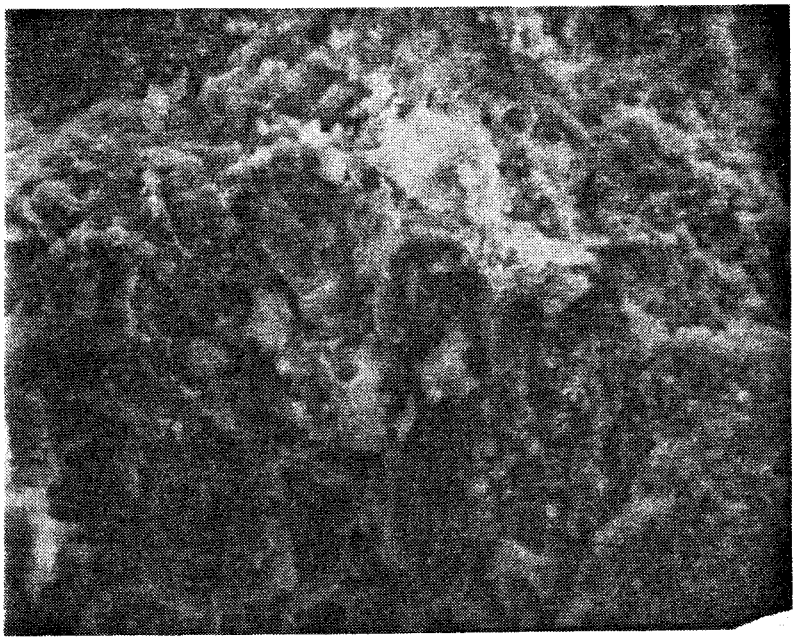

500 X

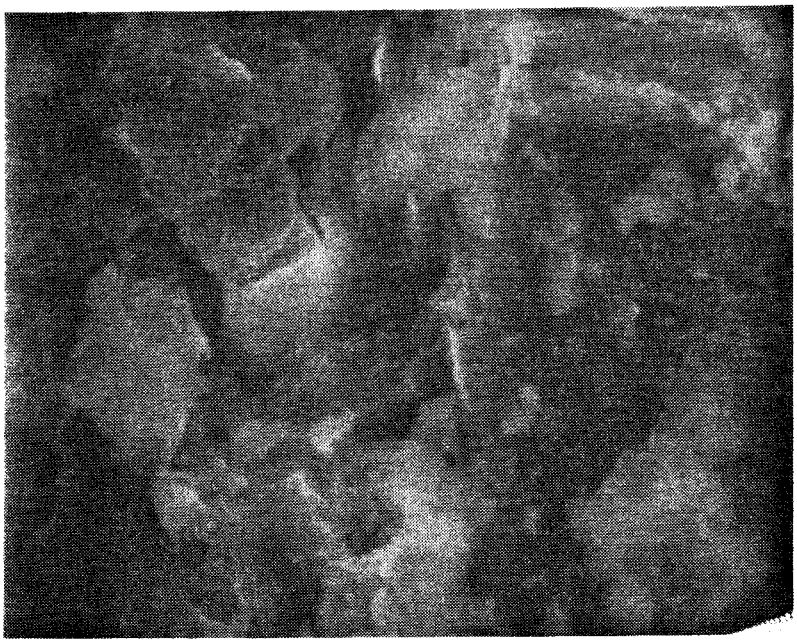

1500 X

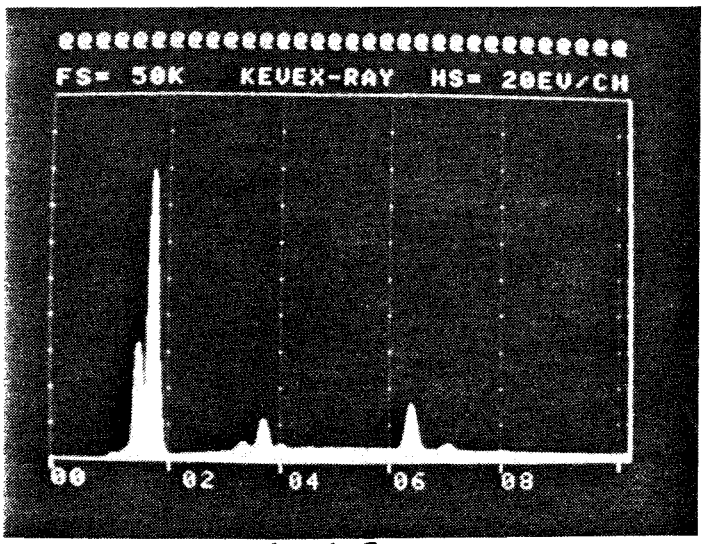

SMALL AREA SCAN @ 1500 X

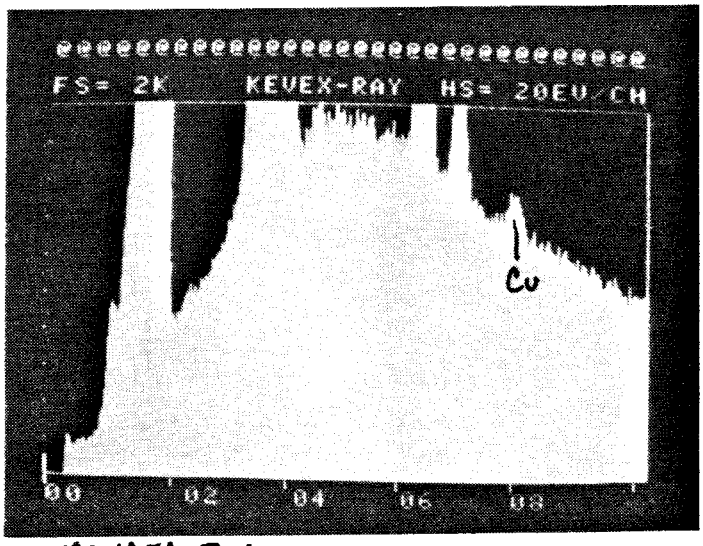

EXPANDED SCALE

SAMPLE: C-a

RUN: 2

POSITION: 0.3 mm

PLATE 7

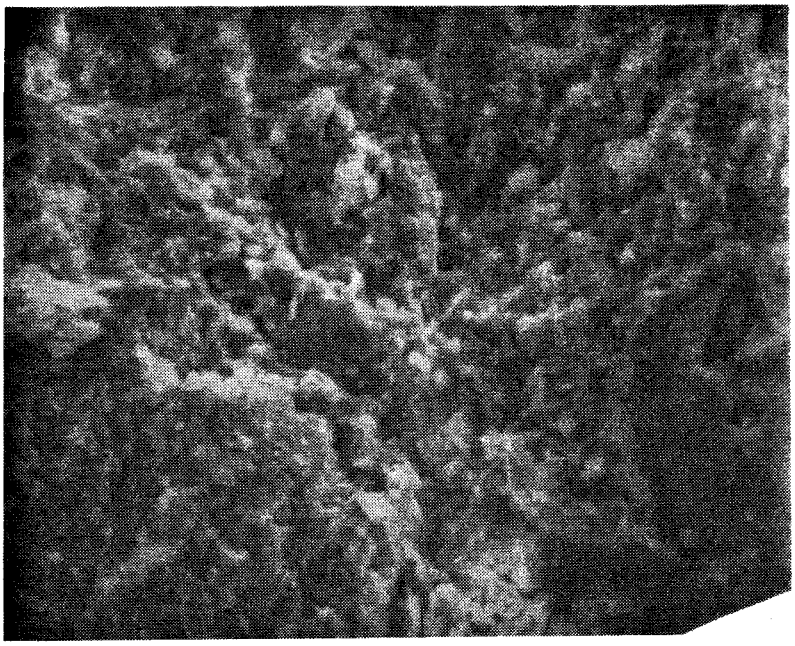

500 X

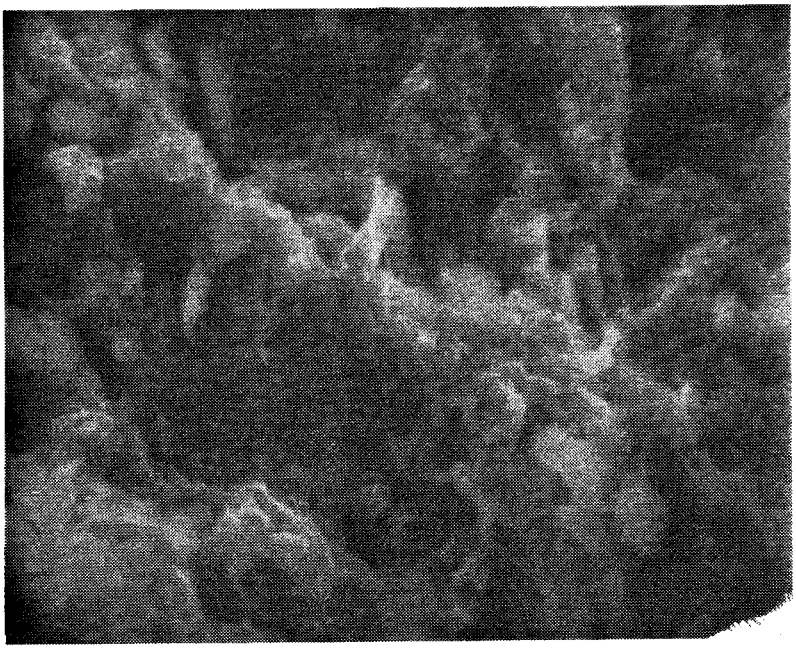

1500 X

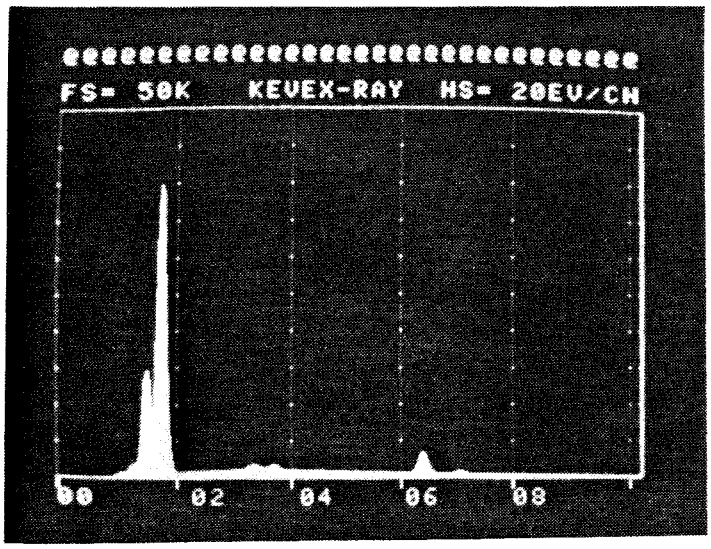

SMALL AREA SCAN @ 1500 X

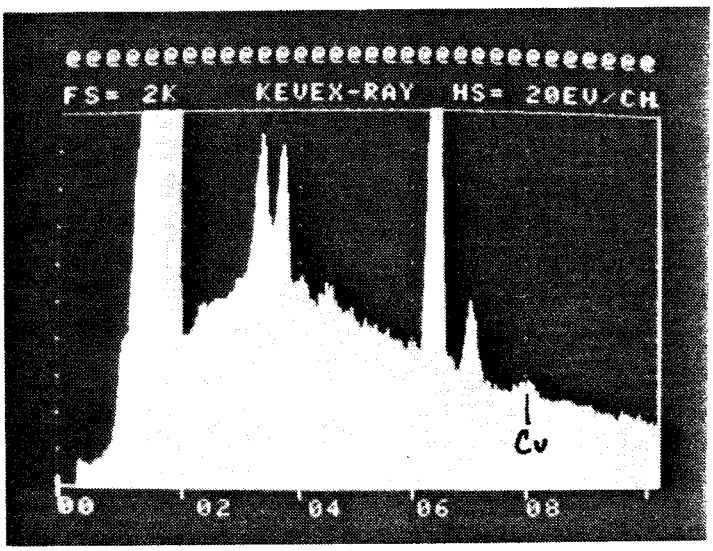

EXPANDED SCALE

POSITION: 0.4 mm

SAMPLE: C-a

PLATE 8

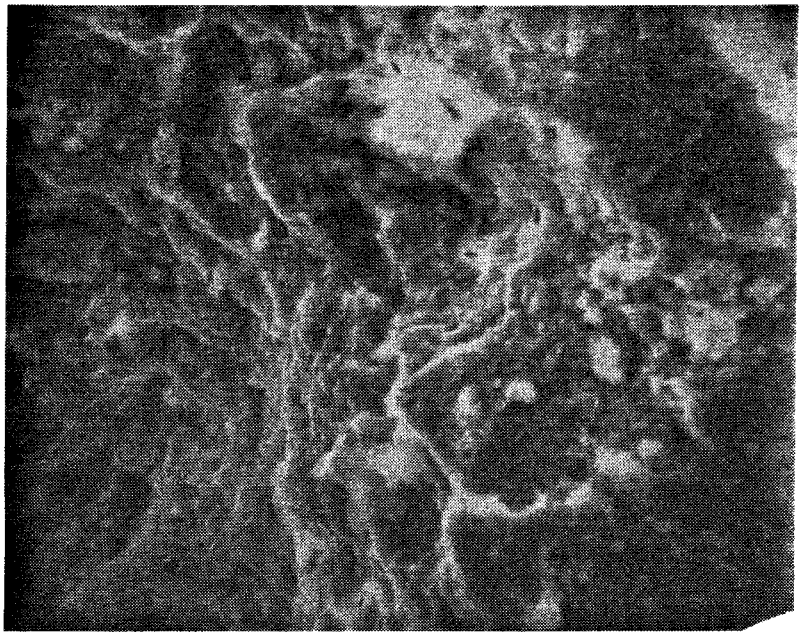

500 X

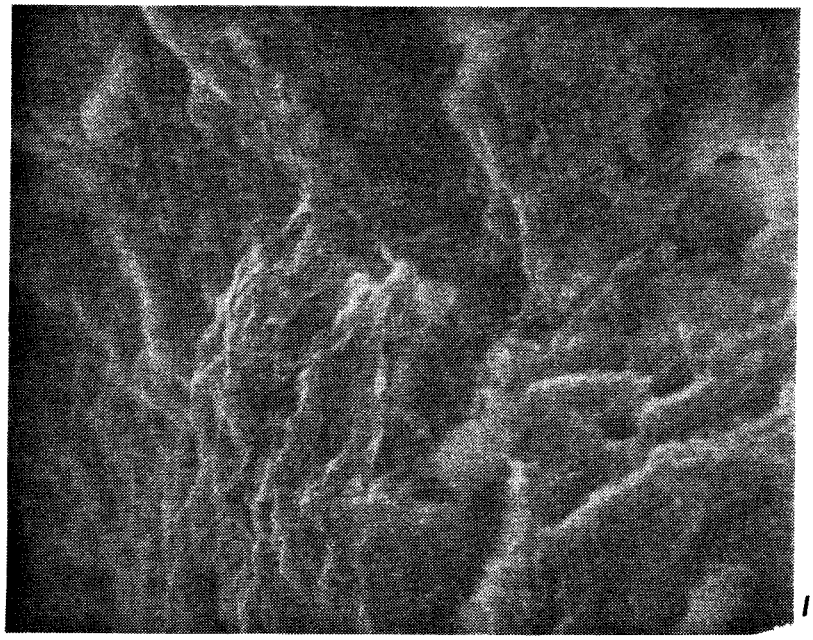

1500 X

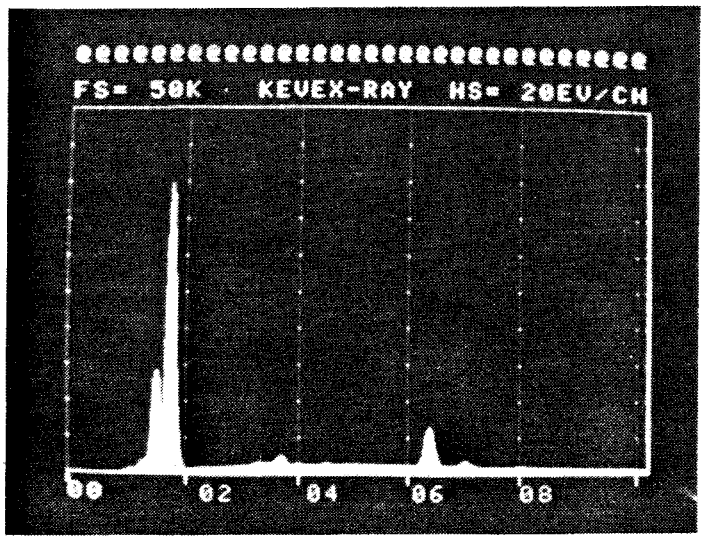

SMALL AREA SCAN @ 1500 X

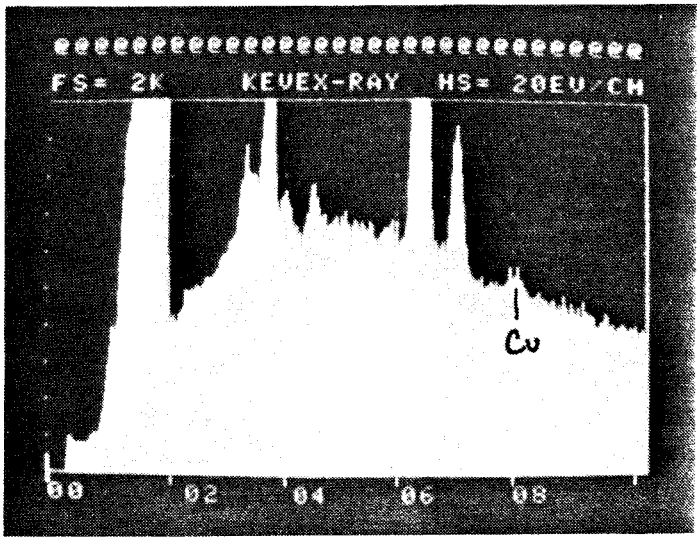

EXPANDED VIEW

POSITION: 1 mm

SAMPLE: C-a

PLATE 9

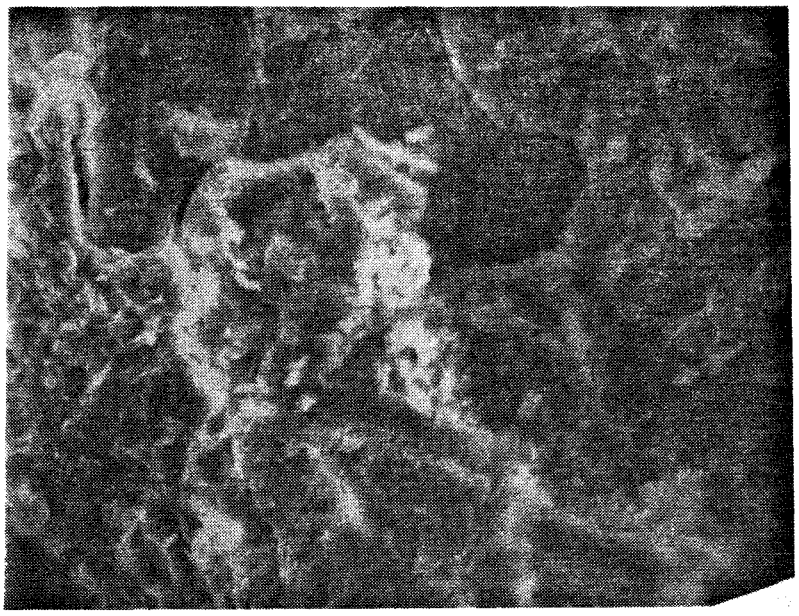

500 X

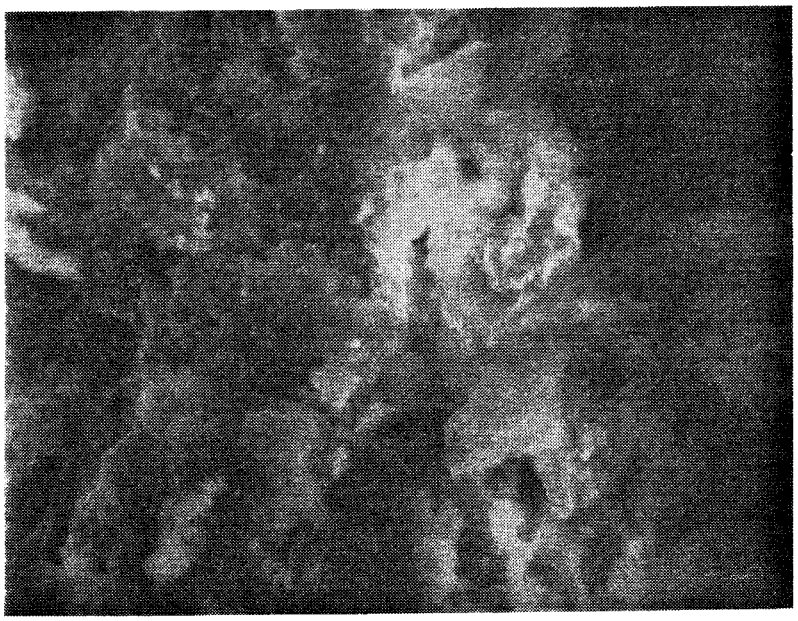

1500 X

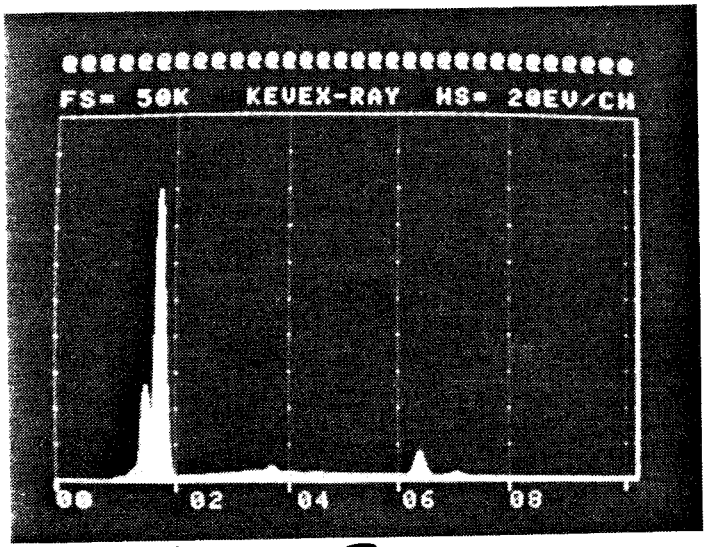

SMALL AREA SCAN @ 1500X

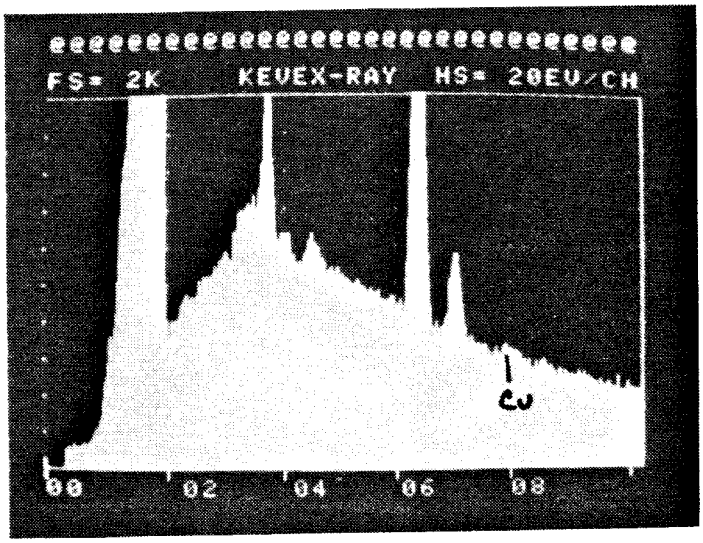

EXPANDED VIEW

SAMPLE: C-a
RUN: 2

POSITION: 2 mm

APPENDIX 2

ELEMENT ANALYSES (EMV)

PLATES 10-19

NOTE B: OFF-EDGE RESPONSE IS DUE TO "LEDGE" OF CLAY PROJECTING OUT AT A LEVEL LOWER THAN THE FRACTURE SURFACE.

AL = ANALYSIS LINE
FS = FULL SCALE
CPS = COUNTS PER SECOND

SAMPLE: C-r
RUN: 1

LINE ANALYSIS
FS SENSITIVITY: 1.0×10^2 CPS
SCAN SETTING: 6

MAP
SCAN SETTING: 10

NOTE A: DATA IN THIS REGION UNRELIABLE DUE TO DETECTOR SATURATION. SEE SCAN OF SAME REGION AT REDUCED SENSITIVITY (SEPARATE PAGE). ALSO SEE RUN 2, FOR WHICH SAMPLE WAS REVERSED SO THAT DETECTOR SATURATION WOULD OCCUR OFF-SAMPLE.

PLATE 10

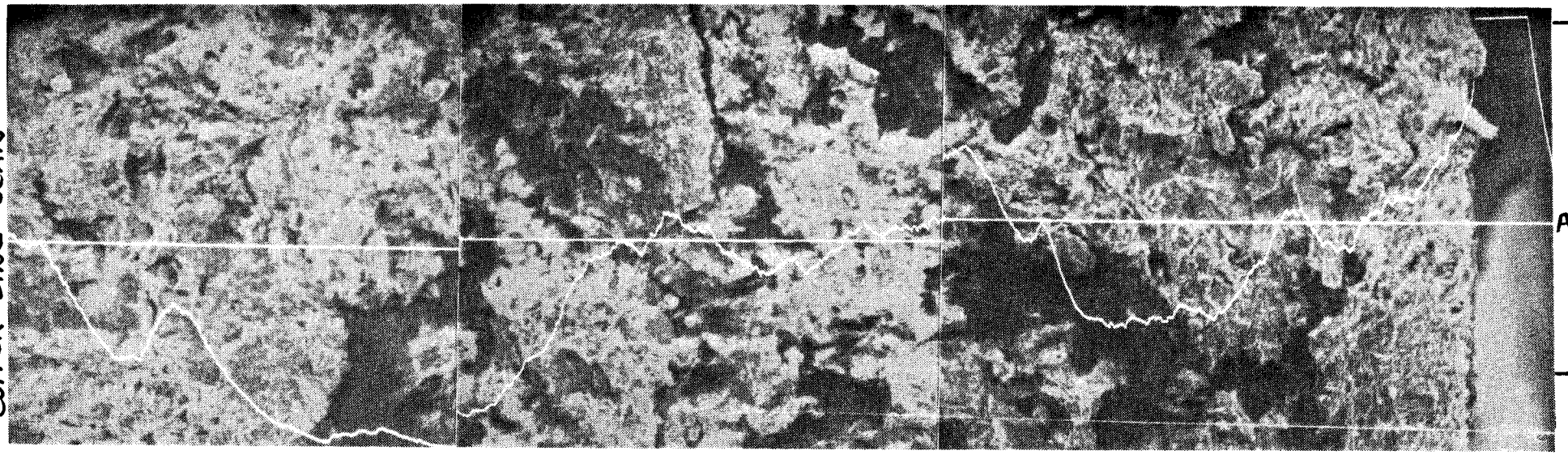

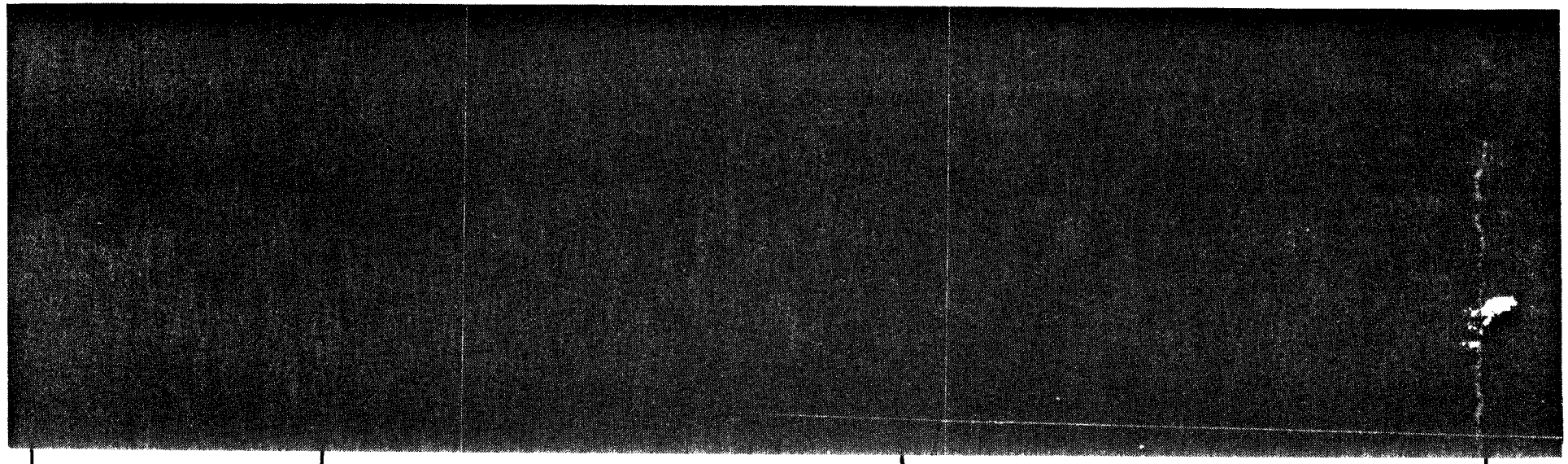

2.5 mm 2 mm 1 mm 0

BEAM TRAVEL →

SAMPLE: C-r
RUN: 2

LINE ANALYSIS
FS SENSITIVITY: 1.0×10^2 CPS
SCAN SETTING: 6

MAP
SCAN SETTING: 10

NOTE: SAMPLE HAS BEEN REVERSED SO THAT DETECTOR SATURATION AT COPPER-RICH INTERFACE OCCURS OFF-SAMPLE. SEE SCAN OF SAME REGION AT REDUCED SENSITIVITY (SEPARATE PAGE).

AL ≡ ANALYSIS LINE
FS ≡ FULL SCALE
CPS ≡ COUNTS PER SECOND

PLATE 11

PLATE 12

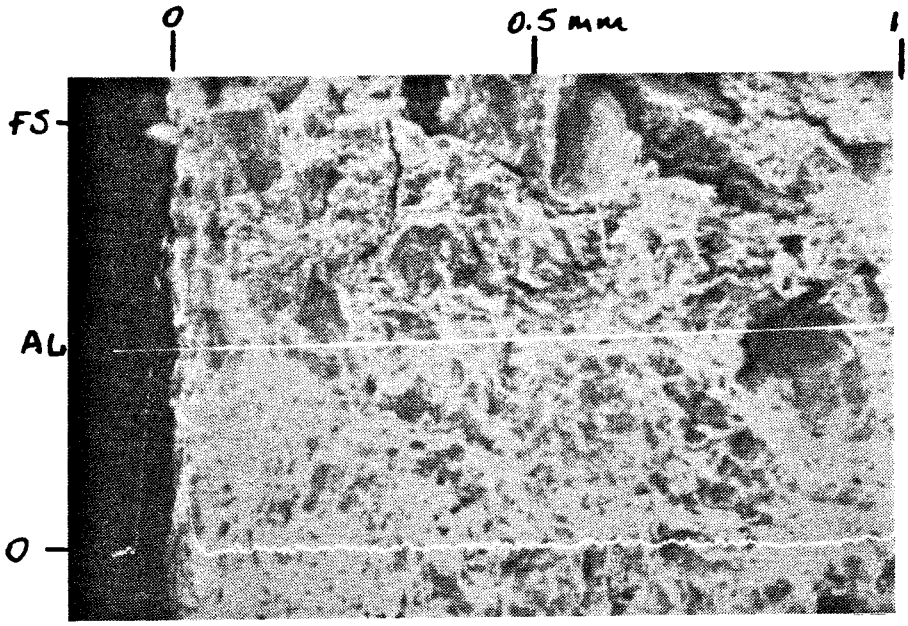

COPPER LINE SCAN OF SAMPLE C-r AT REDUCED SENSITIVITY (2.5×10^3 CPS). COMPARE WITH RUN 1 LINE SCAN AT HIGHER SENSITIVITY.

AL ≡ ANALYSIS LINE

FS ≡ FULL SCALE

CPS ≡ COUNTS PER SECOND

PLATE 13

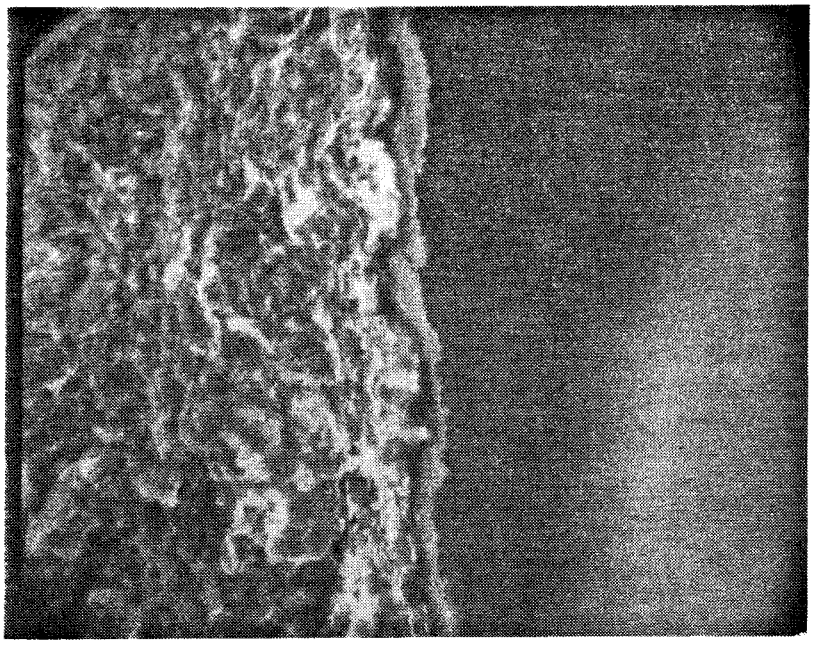

500 X

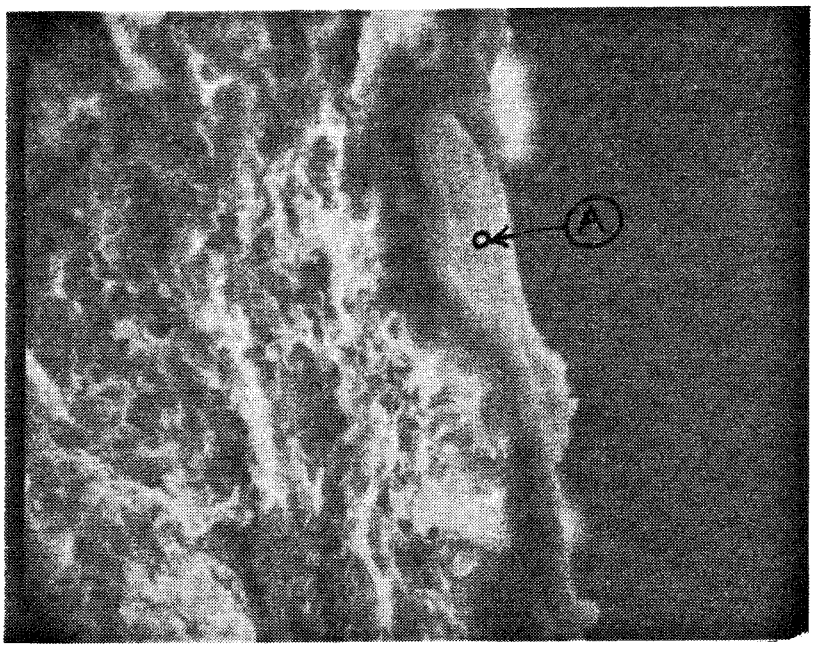

1500 X

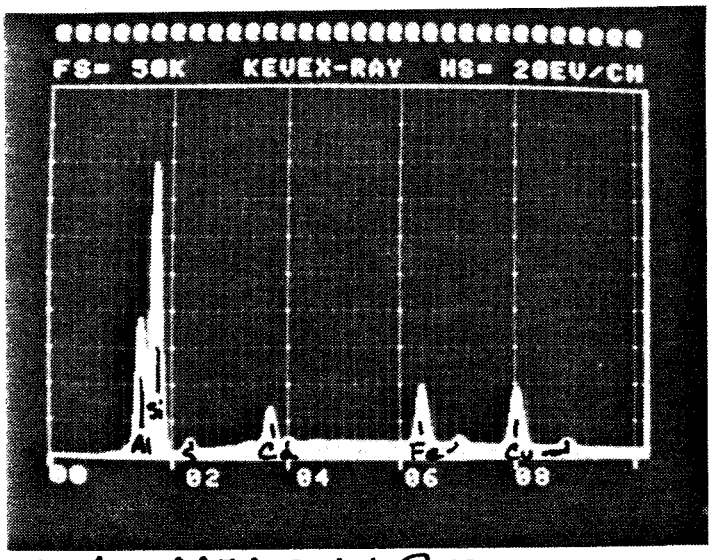

SMALL AREA SCAN @ 1500 X

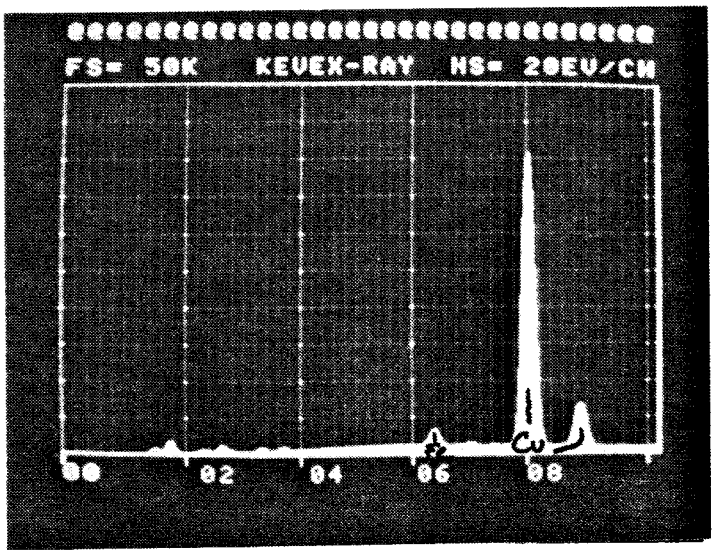

SPOT ANALYSIS OF SURFACE MATERIAL (POINT "A")

SAMPLE: C-1

RUN: 2

POSITION: AT INTERFACE

PLATE 14

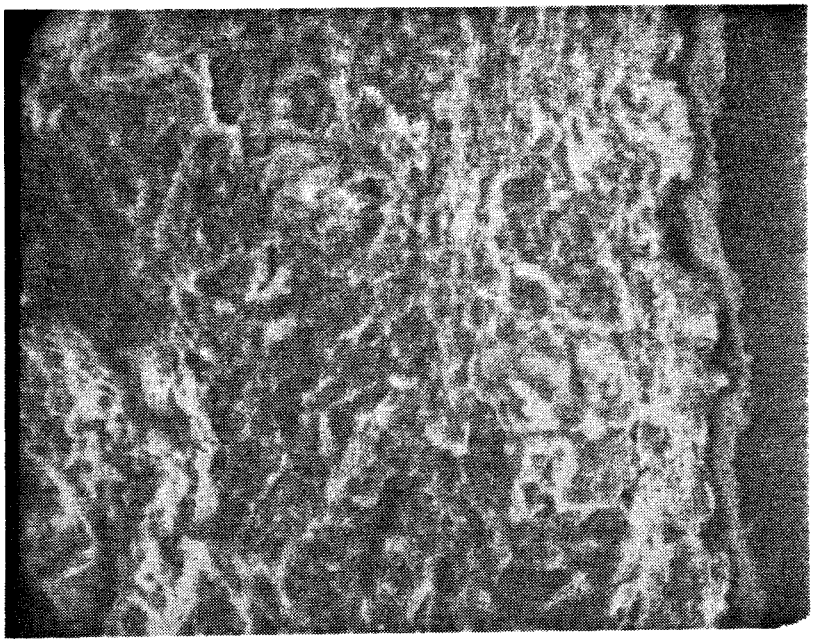

500 X

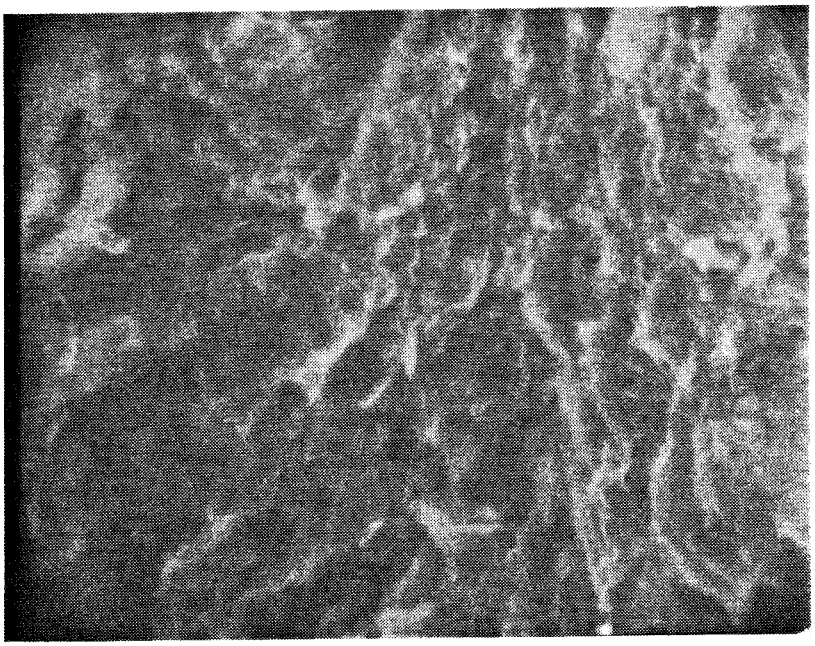

1500 X

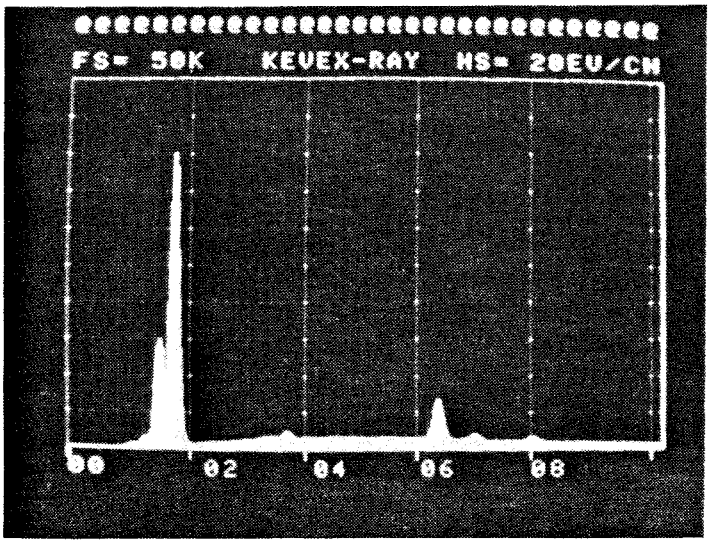

SMALL AREA SCAN @ 1500 X

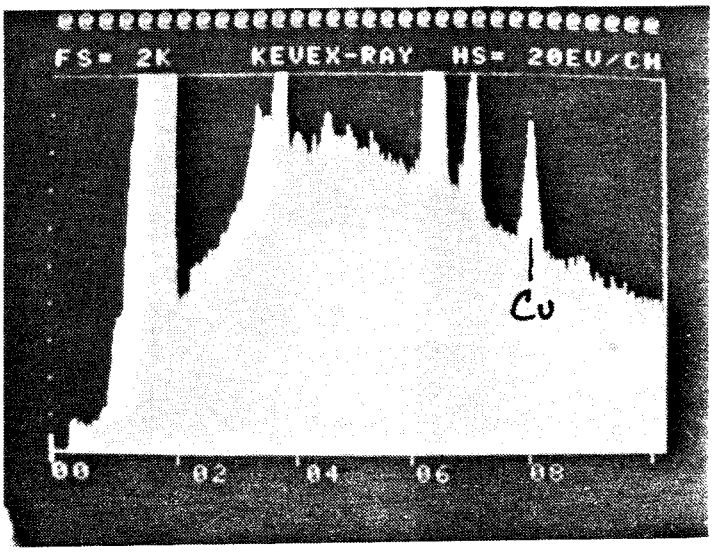

EXPANDED SCALE

SAMPLE: C-r

RUN: 2

POSITION: 0.1 mm

PLATE 15

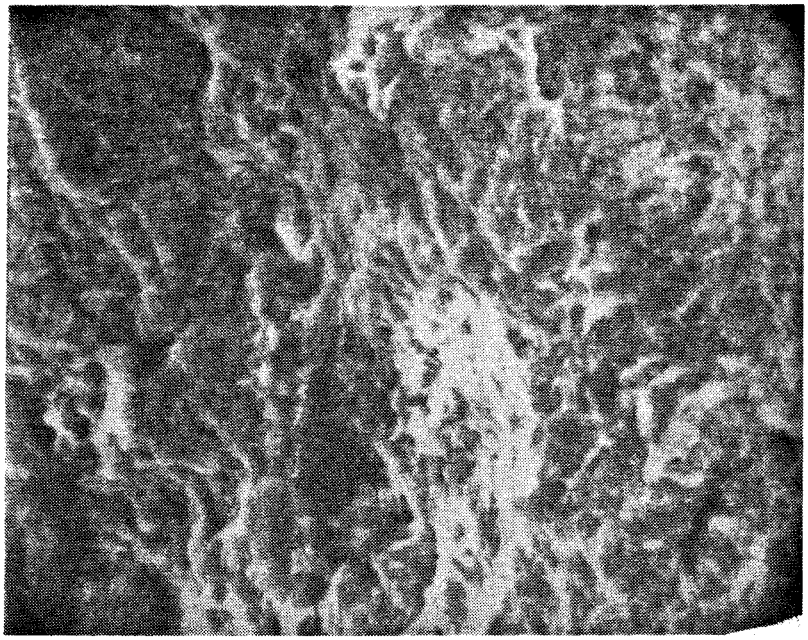

500 X

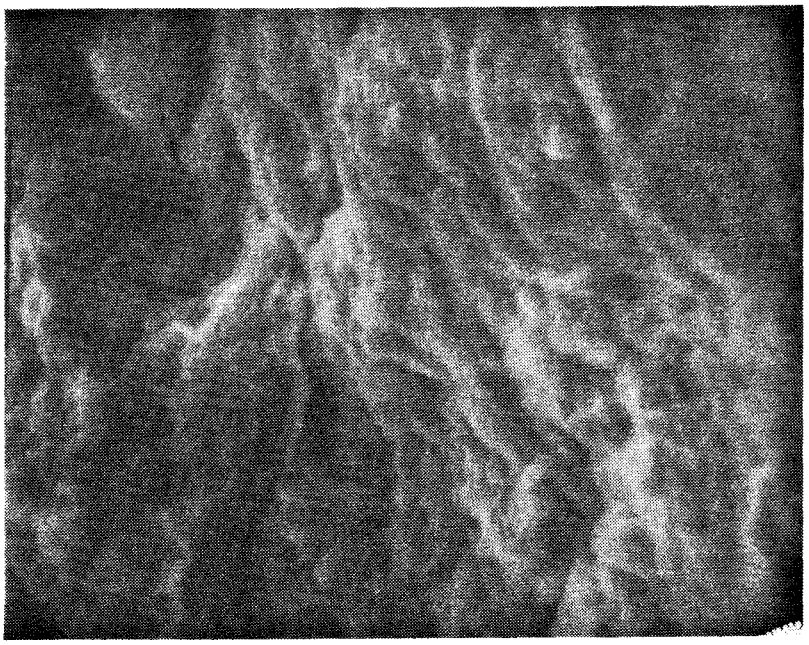

1500 X

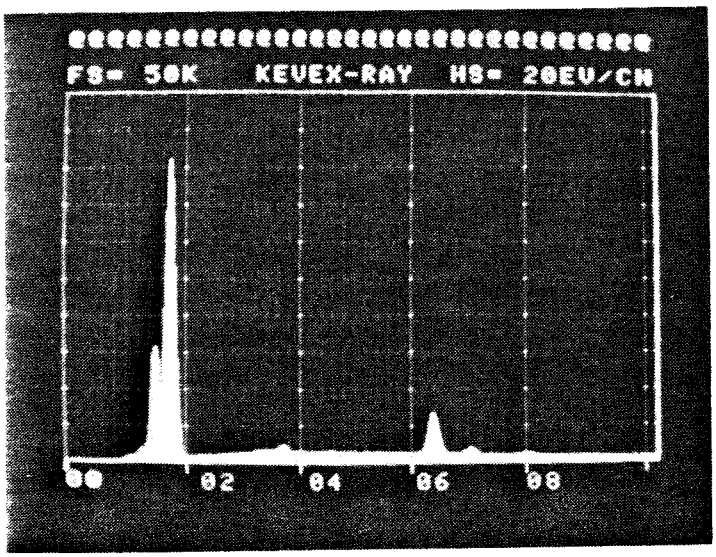

SMALL AREA SCAN @ 1500 X

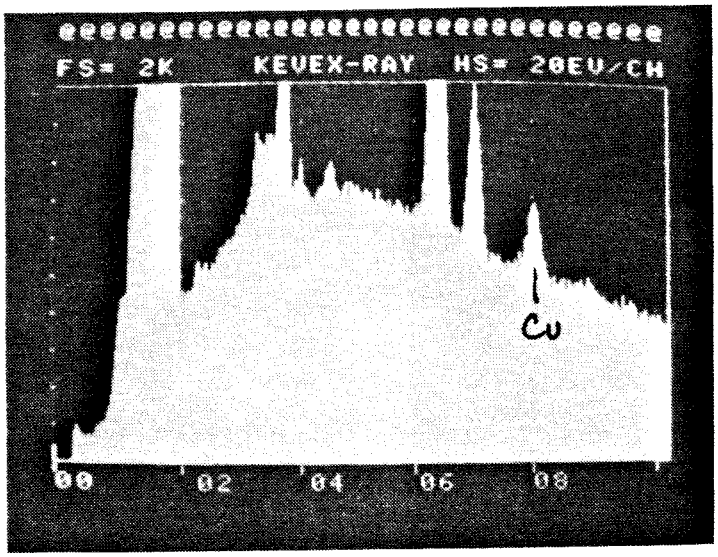

EXPANDED SCALE

SAMPLE: C-r

RUN: 2

POSITION: 0.2 mm

PLATE 16

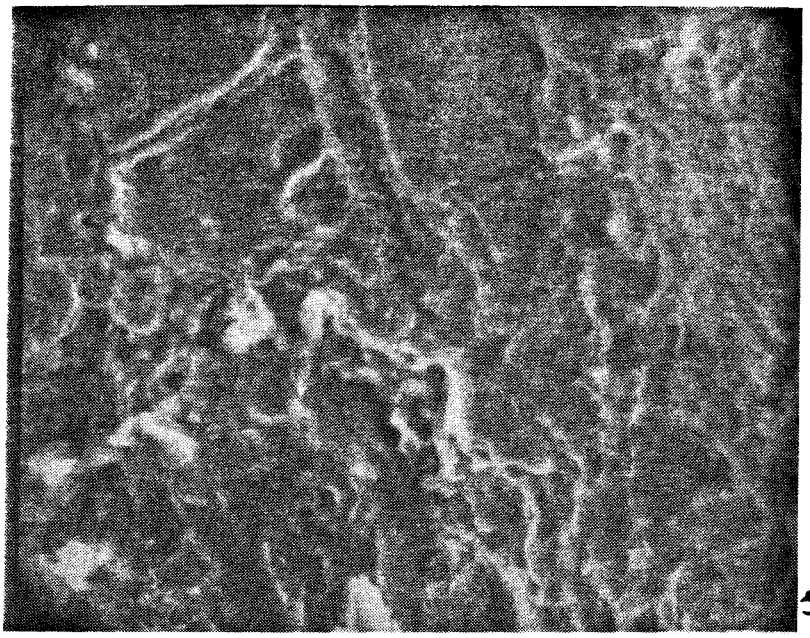

500 X

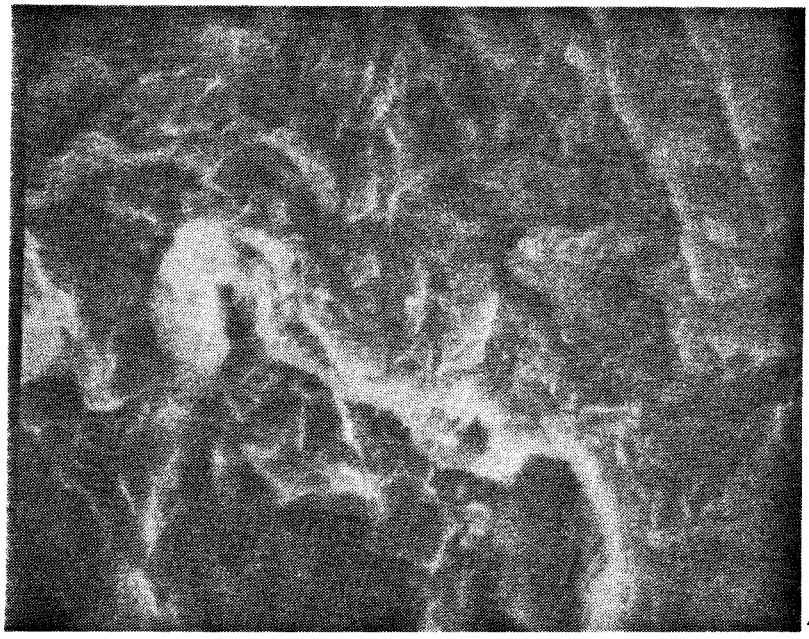

1500 X

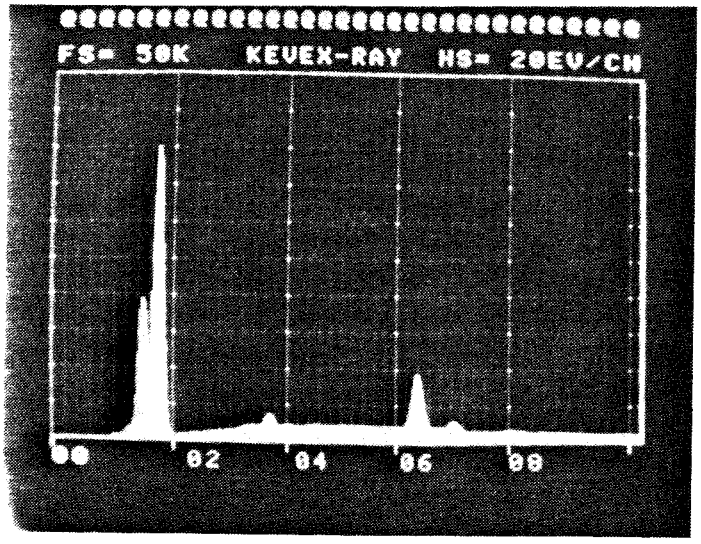

SMALL AREA SCAN @ 1500X

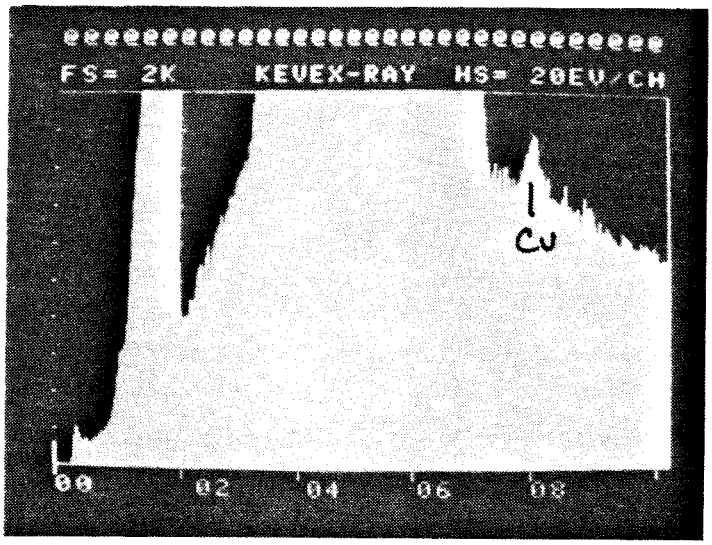

EXPANDED SCALE

POSITION: 0.3 mm

SAMPLE: C-F

RUN: 2

PLATE 17

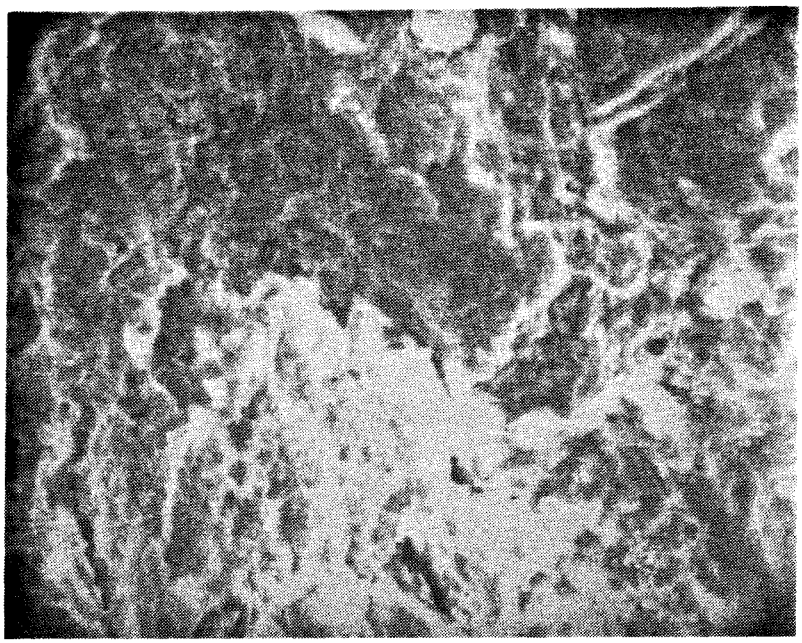

500 X

1500 X

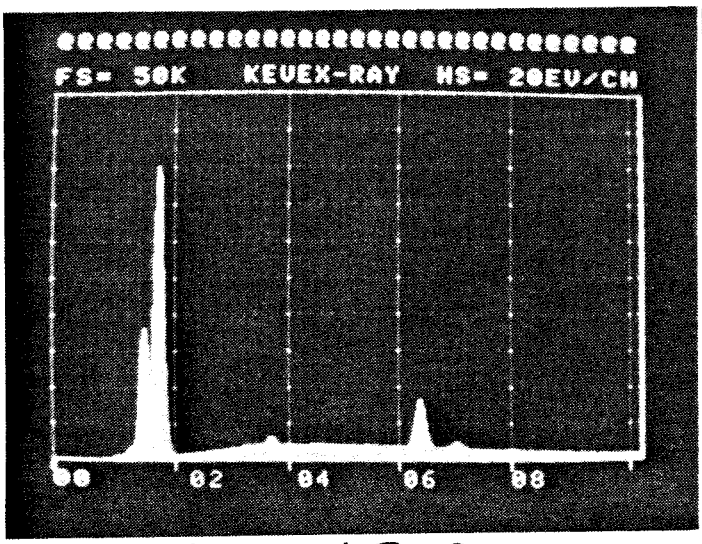

SMALL AREA SCAN @ 1500 X

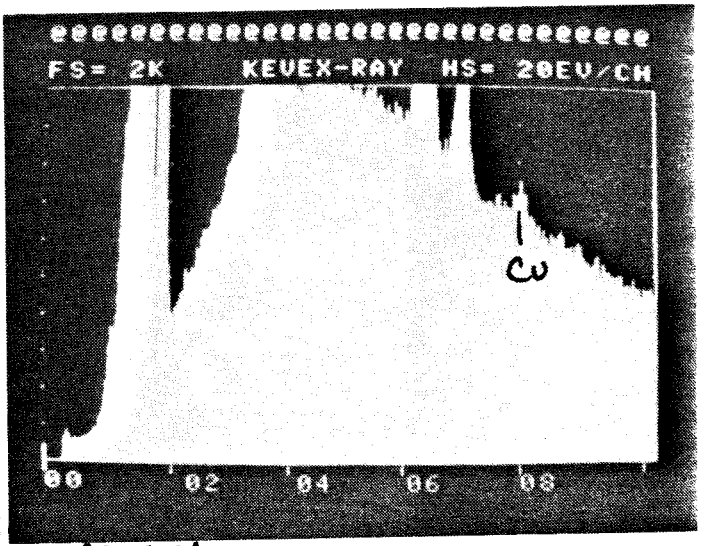

EXPANDED SCALE

SAMPLE: C-P

RUN: 2

POSITION: 0.4 mm

PLATE 18

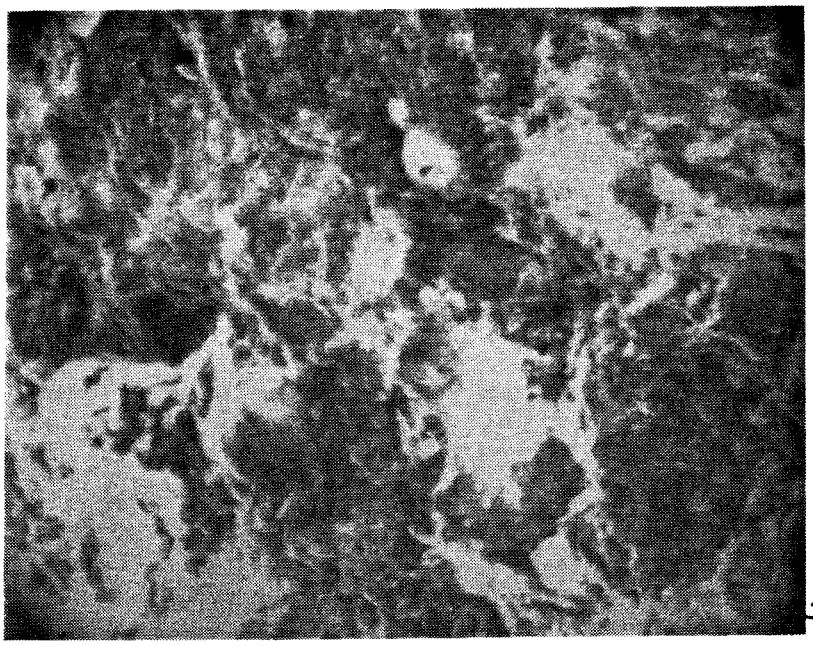

500 X

1500 X

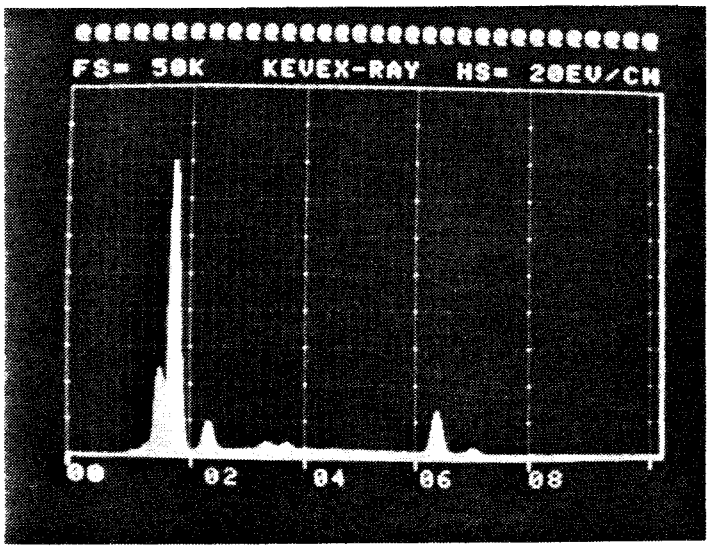

SMALL AREA SCAN @ 1500 X

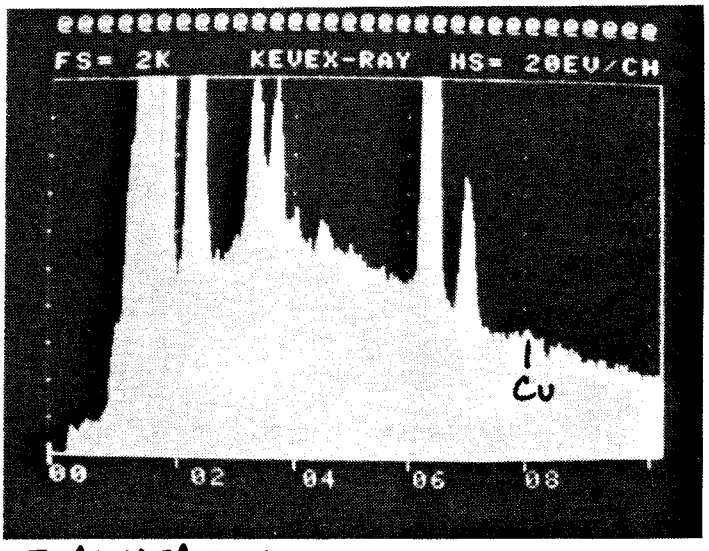

EXPANDED SCALE

SAMPLE: C-r

RUN: 2

POSITION: 1 mm

PLATE 19

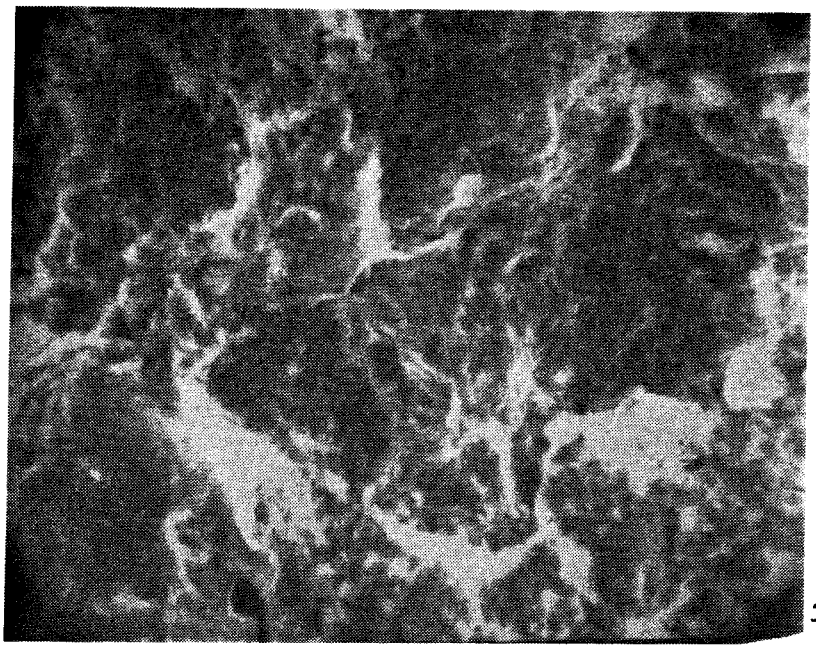

500X

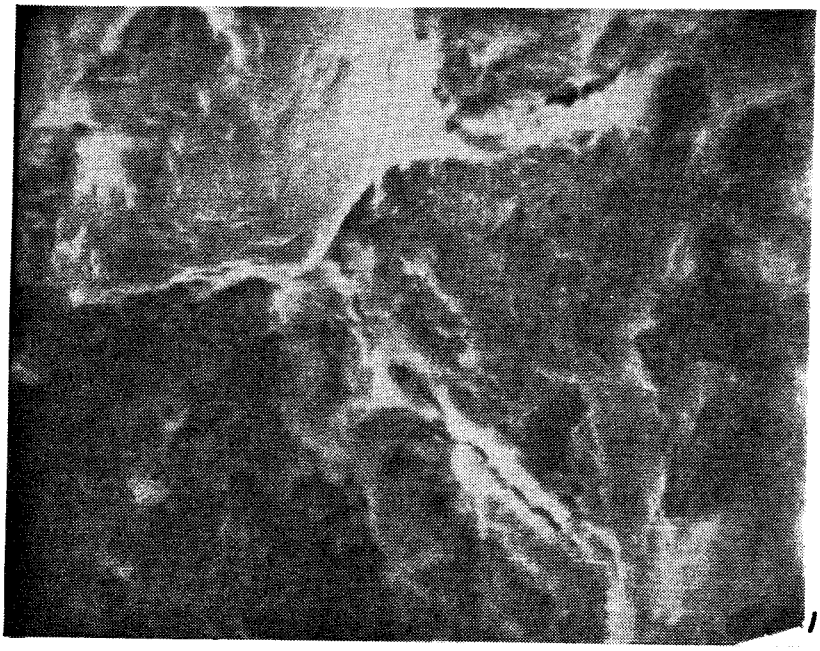

1500X

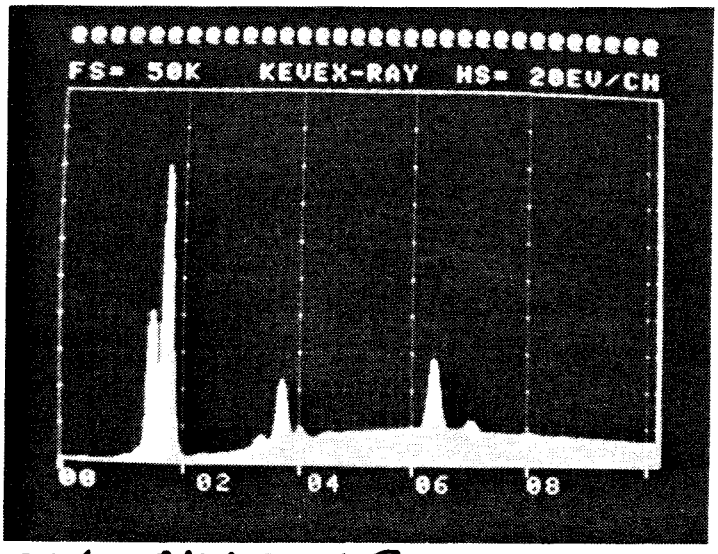

SMALL AREA SCAN @ 1500X

POSITION: 2 mm

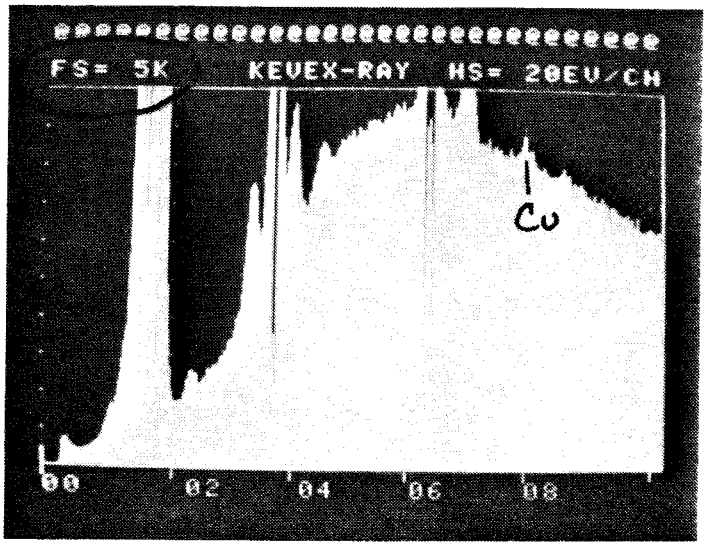

EXPANDED SCALE (NOTE: FULL SCALE IS 5,000 COUNTS, RATHER THAN 2,000 USED FOR ALL OTHER EXPANDED VIEWS. REASON: UNUSUALLY HIGH BACKGROUND LEVEL.)

FÖRTECKNING ÖVER KBS TEKNISKA RAPPORTER

1977-78

TR 121 KBS Technical Reports 1 - 120.
Summaries. Stockholm, May 1979.

1979

TR 79-28 The KBS Annual Report 1979.
KBS Technical Reports 79-01--79-27.
Summaries. Stockholm, March 1980.

1980

TR 80-26 The KBS Annual Report 1980.
KBS Technical Reports 80-01--80-25.
Summaries. Stockholm, March 1981.

1981

TR 81-17 The KBS Annual Report 1981.
KBS Technical Reports 81-01--81-16
Summaries. Stockholm, April 1982.

1982

TR 82-01 Hydrothermal conditions around a radioactive waste repository
Part 3 - Numerical solutions for anisotropy
Roger Thunvik
Royal Institute of Technology, Stockholm, Sweden
Carol Braester
Institute of Technology, Haifa, Israel
December 1981

TR 82-02 Radiolysis of groundwater from HLW stored in copper canisters
Hilbert Christensen
Erling Bjergbakke
Studsvik Energiteknik AB, 1982-06-29

TR 82-03 Migration of radionuclides in fissured rock:
Some calculated results obtained from a model based on the concept of stratified flow and matrix diffusion
Ivars Neretnieks
Royal Institute of Technology
Department of Chemical Engineering
Stockholm, Sweden, October 1981

TR 82-04 Radionuclide chain migration in fissured rock -
The influence of matrix diffusion
Anders Rasmuson *
Akke Bengtsson **
Bertil Grundfelt **
Ivars Neretnieks *
April, 1982

* Royal Institute of Technology
Department of Chemical Engineering
Stockholm, Sweden

** KEMAKTA Consultant Company
Stockholm, Sweden

TR 82-05 Migration of radionuclides in fissured rock -
Results obtained from a model based on the concepts of hydrodynamic dispersion and matrix diffusion
Anders Rasmuson
Ivars Neretnieks
Royal Institute of Technology
Department of Chemical Engineering
Stockholm, Sweden, May 1982

TR 82-06 Numerical simulation of double packer tests
Calculation of rock permeability
Carol Braester
Israel Institute of Technology, Haifa, Israel
Roger Thunvik
Royal Institute of Technology
Stockholm, Sweden, June 1982

TR 82-07 Copper/bentonite interaction
Roland Pusch
Division Soil Mechanics, University of Luleå
Luleå, Sweden, 1982-06-30

TR 82-08 Diffusion in the matrix of granitic rock
Field test in the Stripa mine
Part 1
Lars Birgersson
Ivars Neretnieks
Royal Institute of Technology
Department of Chemical Engineering
Stockholm, Sweden, July 1982